Mannen *et al. Earth, Planets and Space* (2018) 70:68
https://doi.org/10.1186/s40623-018-0844-2

Earth, Planets and Space

FULL PAPER

Open Access

Chronology of the 2015 eruption of Hakone volcano, Japan: geological background, mechanism of volcanic unrest and disaster mitigation measures during the crisis

Kazutaka Mannen[1*], Yohei Yukutake[1], George Kikugawa[1], Masatake Harada[1], Kazuhiro Itadera[1] and Jun Takenaka[2]

Abstract

The 2015 eruption of Hakone volcano was a very small phreatic eruption, with total erupted ash estimated to be in the order of only 10^2 m^3 and ballistic blocks reaching less than 30 m from the vent. Precursors, however, had been recognized at least 2 months before the eruption and mitigation measures were taken by the local governments well in advance. In this paper, the course of precursors, the eruption and the post-eruptive volcanic activity are reviewed, and a preliminary model for the magma-hydrothermal process that caused the unrest and eruption is proposed. Also, mitigation measures taken during the unrest and eruption are summarized and discussed. The first precursors observed were an inflation of the deep source and deep low-frequency earthquakes in early April 2015; an earthquake swarm then started in late April. On May 3, steam wells in Owakudani, the largest fumarolic area on the volcano, started to blowout. Seismicity reached its maximum in mid-May and gradually decreased; however, at 7:32 local time on June 29, a shallow open crack was formed just beneath Owakudani as inferred from sudden tilt change and InSAR analysis. The same day mud flows and/or debris flows likely started before 11:00 and ash emission began at about 12:30. The volcanic unrest and the eruption of 2015 can be interpreted as a pressure increase in the hydrothermal system, which was triggered by magma replenishment to a deep magma chamber. Such a pressure increase was also inferred from the 2001 unrest and other minor unrests of Hakone volcano during the twenty-first century. In fact, monitoring of repeated periods of unrest enabled alerting prior to the 2015 eruption. However, since open crack formation seems to occur haphazardly, eruption prediction remains impossible and evacuation in the early phase of volcanic unrest is the only way to mitigate volcanic hazard.

Keywords: Hakone, Phreatic eruption, Lahar, Debris flow, Ash fall, Fumarole

Introduction

Phreatic eruptions are caused by a violent expansion of steam without direct involvement of magma (e.g., Barberi et al. 1992). Unfortunately, precursors of phreatic eruptions are often subtle or useless, even at well-observed volcanoes (e.g., Jolly et al. 2010). On the other hand, all around the world, sites of potential phreatic eruptions often form major tourist destinations for their peculiar landscape and scenery. The proximity of people to eruption centers and subtle precursors of phreatic eruptions have led to tragedies, with the 2014 eruption of Ontake volcano the latest example (Maeno et al. 2016). However, the 2014 Ontake eruption had subtle but detectable preparatory processes, such as inflation of deep and shallow

*Correspondence: mannen@onken.odawara.kanagawa.jp
[1] Hot Springs Research Institute of Kanagawa Prefecture, 586 Iriuda, Odawara, Kanagawa 250-0031, Japan
Full list of author information is available at the end of the article

sources (Miyaoka and Takagi 2016; Murase et al. 2016) and earthquakes in the conduit system (Kato et al. 2015). These observations suggest that adequate monitoring and modeling could pave the way for success in alerting of phreatic eruption well in advance.

Hakone volcano had no historical record of eruption before 2015; however, frequent earthquake swarms had concerned local people. Due to its proximity to the capital city of Tokyo, and plentiful hot spring resources, Hakone is one of the most popular resort areas in Japan and approximately twenty million tourists visit every year. Concerned about eruptions, the local government has deployed seismological and geodetic instruments in and around the volcano since 1960. In the past two decades, Hakone has been active in terms of seismicity and crustal deformation and a model of the magma-hydrothermal system of the volcano has been proposed (Mannen 2008). In addition, major volcanic unrest in 2001 prompted establishment of a mitigation plan by local governments. Under this circumstance, the 2015 eruption occurred.

Owing to the reasonably equipped monitoring system, the volcanic activities before, during and after the eruption were observed well, and a geophysical model of the eruption was established even though the eruption was very small. Also, the pre-established mitigation plan enabled the ability to set a no-entry zone long before the eruption and human damage was therefore avoided. We consider that our experience can help improve future monitoring and mitigation plans not only of Hakone volcano, but of other hydrothermal-prone volcanoes. In this paper, general geological and geophysical studies of Hakone volcano are reviewed and a chronology of the 2015 eruption is summarized. Based on this knowledge, mechanisms that caused the precursor unrest and eruption will be discussed.

Geological setting

General geology

Hakone volcano is an active volcano located on the volcanic front in the central part of Honshu Island, Japan (Fig. 1a). The volcano has an eruptive history of more than 400 ka as implied from K–Ar dating and tephrochronological studies (Hakamata et al. 2005; Oikawa and Ishizuka 2011). The topography of the volcano is shown in Fig. 1b. Hakone is a caldera volcano with a complex of stratovolcanoes of basaltic to andesitic composition forming the caldera rim ($\geq$ 230 ka). Within the caldera, central cones have been formed. The caldera seems to have been formed by multiple pumice flow events in 230–130 ka and 80–40 ka. The volume of each pumice flow event is estimated to have been in the order of 10 km^3 (Machida and Arai 2003).

The central cones are classified based on their ages: older central cones mainly composed of andesite to rhyolite magmas (130–80 ka), and younger central cones composed of compositionally monotonous andesite (40 ka to the present).

For the younger central cones, 12 magmatic events of block and ash flow are recognized up to the present. Among them, the youngest event, which formed a lava dome named Kanmurigatake, occurred 3 ka in the northern part of the younger central cones (Kobayashi 1999). This eruption seems to have triggered a sector collapse of the northern part of the central cones. Located in the eastern part of the amphitheater formed by this sector collapse is Owakudani, the area of the 2015 Hakone eruption (Fig. 1b).

Following the youngest magmatic eruption, 6 phreatic eruptions are recognized in the Owakudani area based on tephra deposits (Kobayashi et al. 2006; Tsuchiya et al. 2017). These phreatic eruptions were accompanied by ash falls and debris flows. In addition, ballistic ejecta and surge deposits were distributed in the proximal area (Kobayashi et al. 2006; Tsuchiya et al. 2017). The individual erupted volumes are estimated to be in the order of 10^5 m^3.

Historical unrests

The most recent phreatic eruption prior to 2015 dates to the twelfth–thirteenth century as implied from radiocarbon dating and tephrochronology (Kobayashi et al. 2006); however, there are no historical documents that record the eruption. On the other hand, there is a document that describes an earthquake swarm at the volcano in AD 1786, which caused slight damage to buildings and a near-panic situation in local communities, although there were no injuries or death toll (Ishibashi 1993). The magnitude of the largest earthquake in this event was estimated to be $M = 5.0$–5.5 by an isoseismal method (Usami 2003).

An earthquake swarm in 1917 was the first event after AD 1786, and more than 300 earthquakes were felt by residents in Ubako village (Fig. 1b). Based on an isoseismal method and direction analysis of rumble, the central part of the younger central cones was assumed to be the epicenter of the swarm event (Nakamura 1917; Omori 1917). After this event, major earthquake swarms were recorded in 1923, 1933–1935, 1943, 1944, 1952 and 1959–1960 (Mannen 2003). Among them, the earthquake swarm in 1933–1935 was characterized by prolonged geothermal anomalies, including steaming from the central cones. A report of the local meteorological station says a phreatic eruption occurred on February 22 of 1934, although the location of the eruption center is ambiguous and there is no newspaper coverage of the incident

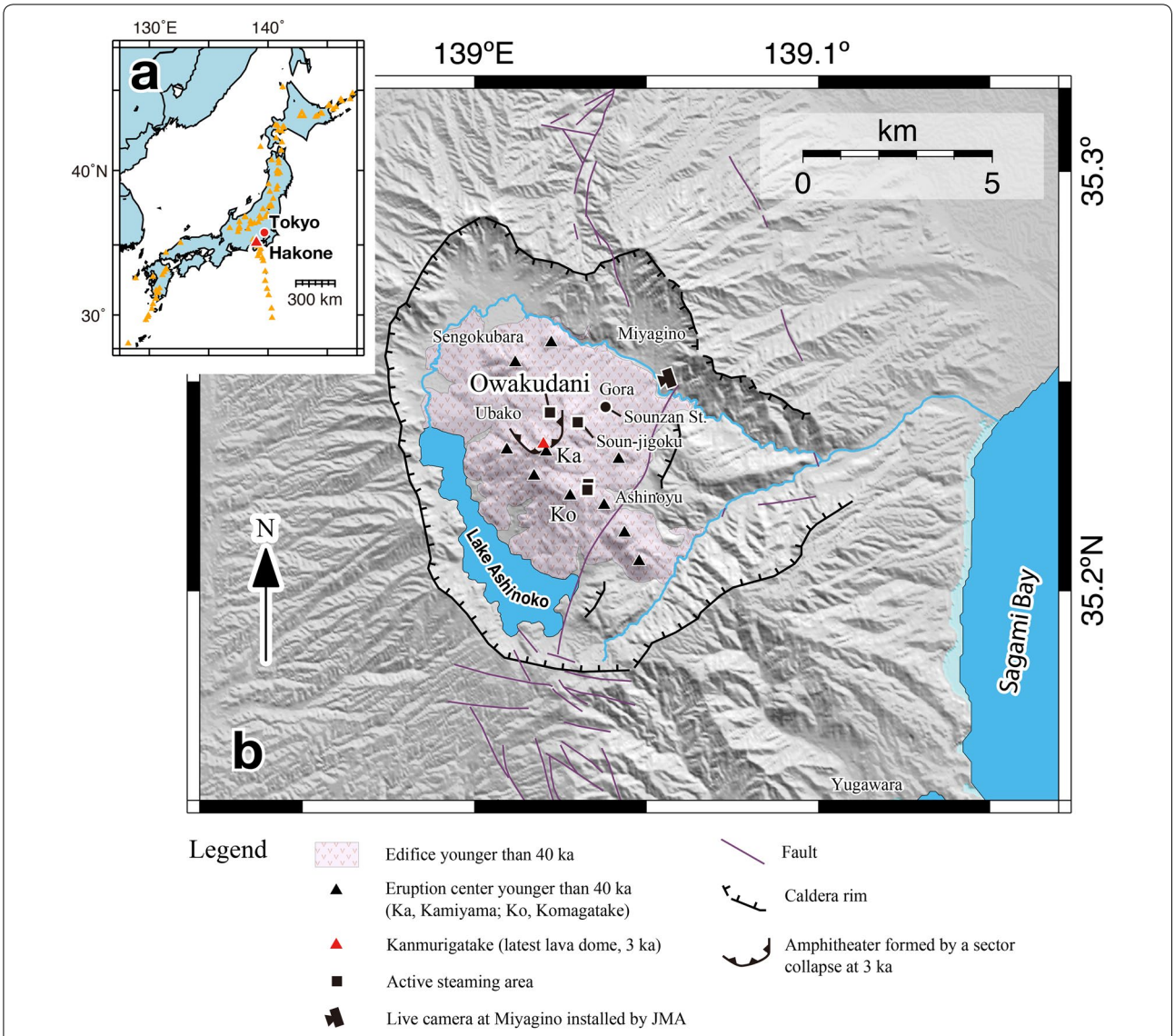

Fig. 1 Index map of Hakone volcano and Owakudani, center of the 2015 eruption. **a** Location of Hakone volcano. Yellow triangle indicates active volcano. **b** Topographical map of Hakone volcano

(Mannen 2003). For the other earthquake swarms, there are some descriptions about anomalies in steaming areas, such as new boiling or more intensive steaming than usual; however, we remain skeptical about these descriptions as they are ambiguous and not deduced from long-term observations.

Geophysical observation

At Hakone volcano, the first instrumental seismic observation was conducted in 1935, although it was a temporary observation and no epicenter was determined. During the 1959–1960 earthquake swarm, four seismometers were deployed in the northern part of the younger central cones area by the Earthquake Research Institute, the University of Tokyo, and this network was then perpetuated by the Kanagawa prefectural government. Since this time, seismic data of uniform quality have been collected continuously, although successive upgrades of the network have gradually improved detection limits and hypocenter accuracies.

Honda et al. (2011) reanalyzed old records taken by the first network and pointed out that epicentral regions of the minor earthquake swarms in 1970s were not significantly different from those detected by the present network. Also, Honda et al. (2011) found a period of seismic

quiescence from the late 1970s to early 1980s, in which only a few earthquakes were recorded in each month.

In 2001, a large and prolonged earthquake swarm occurred. This event accompanied an evident geothermal anomaly and inflations in deep and shallow parts of the volcano, which were the first detected since tilt meters were deployed in 1989 and the GNSS network became operational from 1992. This event is termed the 2001 unrest and will be discussed in detail in a following section.

After this event, there were unrests in 2006, 2008–2009 and 2013, all accompanied by slight inflation of the volcano, the source of which were estimated to be 7–10 km beneath the central part of the volcano (Harada et al. 2009, 2013; Miyaoka et al. 2011). These periods of unrest were more intense than any that occurred after 1960 and before 2001 measured by the magnitude of the largest earthquake, number of earthquakes and duration of events. Since 2001, Hakone volcano is thus likely to be in an active phase (Honda et al. 2011).

Heat flux of steaming area

There are four steaming areas at Hakone volcano (Fig. 1b). Owakudani steaming area is the largest among them and one of the most popular tourist destinations of Hakone area (Fig. 2). The eastern half of the steaming area forms a deep valley named Owakudani (great boiling valley), which is also the name of the region. Within the valley, hot springs are made artificially by mixing steam and pumped water. Most of the steam utilized to make hot springs is obtained from steam production wells (hereafter SPWs), the depth of which are less than 500 m. The production rate of artificial hot springs, or in other words the thermal energy taken from underground, has been monitored once a month for more than 30 years. Also, the underground temperature distribution at 50 cm deep had been measured almost every year and the heat flux to the surface has been calculated (Fig. 3).

As shown in Fig. 3a, the heat flux of Owakudani had decreased in these 3 decades, likely due to a decreasing heat flux of SPWs. This is caused by socioeconomic

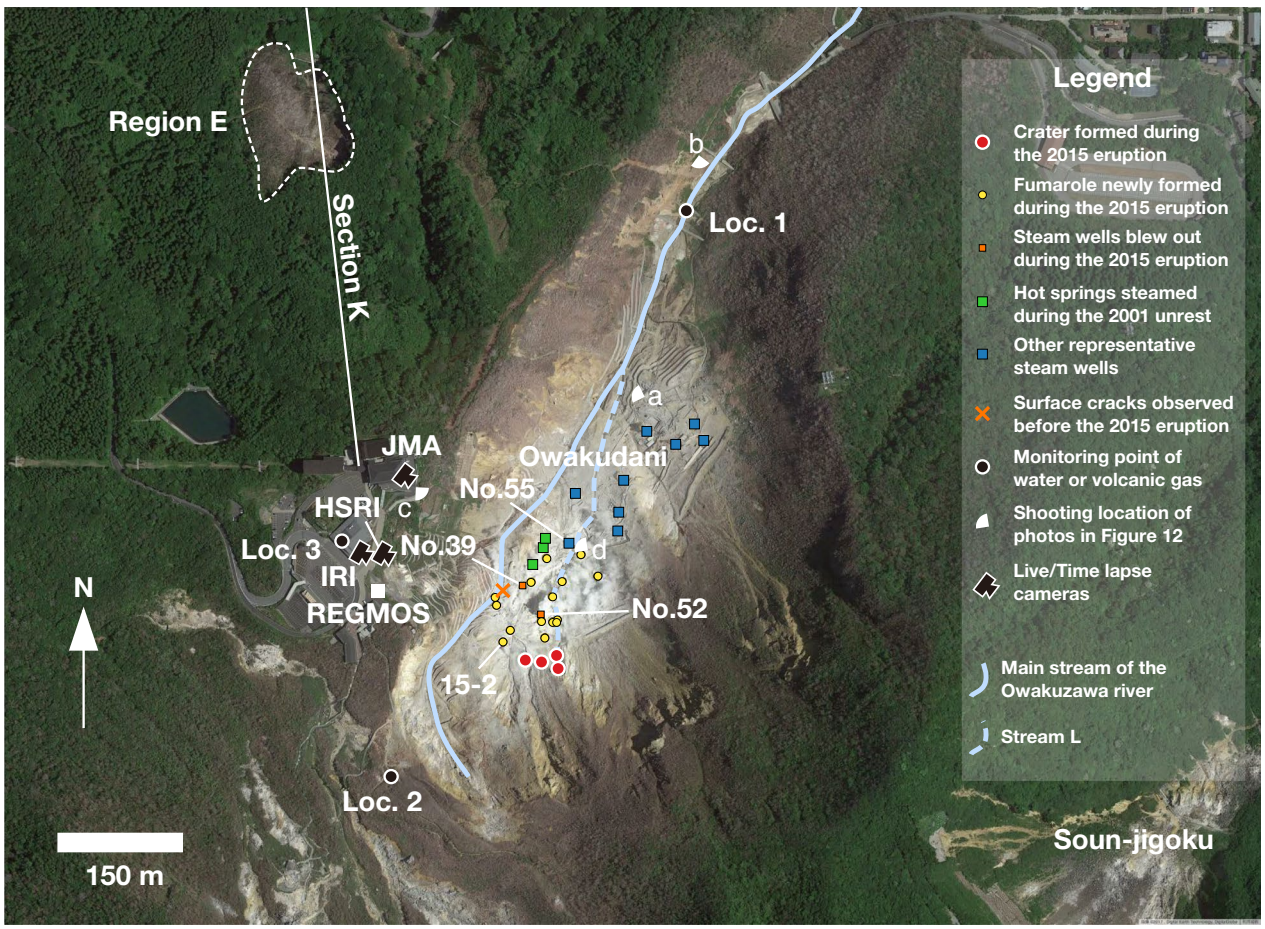

Fig. 2 Aerial photograph of Owakudani and surrounding area (photograph source: Google Earth). Region E indicates a steaming area newly formed in 2011 (see text). Section K indicates a line along which cross-sectional structure of resistivity is shown (Fig. 4)

circumstances: the number of recreation facilities owned by companies, which are the major users of artificial hot springs, has been decreasing due to a prolonged economic recession and users' shifts in preference. Here, non-SPW heat flux, including natural fumaroles, natural hot springs and heat radiation from the ground, is referred to correctively as natural heat flux (NHF).

Temperatures of surface fumaroles in Owakudani have been measured and reported sporadically, mainly when earthquake swarms took place (Table 1). Until the 1930s, some observers reported superheated steams from natural fumaroles; however, since the 1950s, no superheating had been reported until the 2015 eruption. This could be attributed to bypassing of underground geothermal water by the SPWs that started in 1954 (Mannen 2009). In fact, steam production by SPWs seems to have diminished NHF as indicated by a strong negative correlation between NHF and heat flux from SPWs (Fig. 3b).

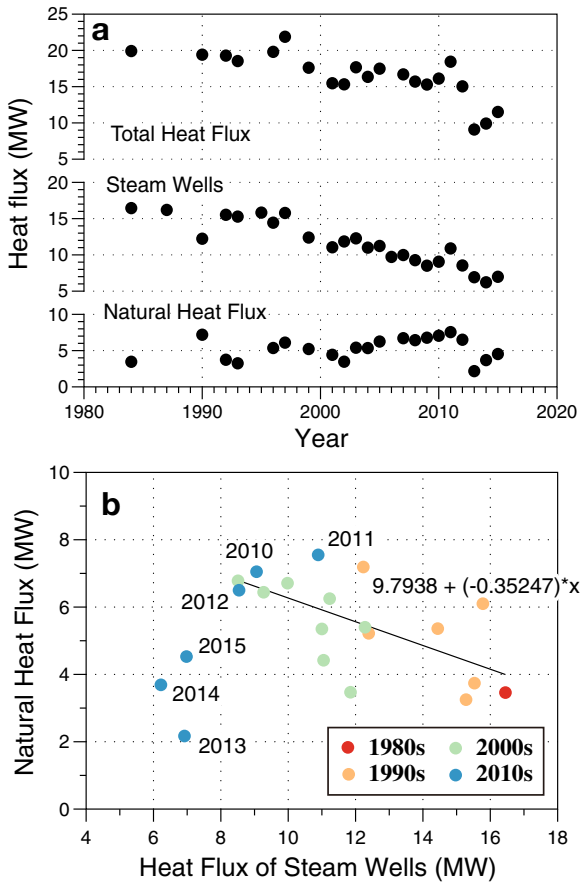

Fig. 3 Heat flux of Owakudani area (1983–2015). **a** Total, steam well and natural heat flux. **b** Relationship between steam well and natural heat fluxes. Note that the heat flux of the steam well has decreased in these three decades almost constantly. On the other hand, natural heat flux has increased. Since only 35% of heat flux reduction in steam wells contributes to the increase in natural heat flux at the ground surface as inferred from the regression line in (**b**), total heat flux is known to decrease with steam well reduction. Observations from 2013 to 2015, which seem to depart significantly from the regression line, infer an altered hydrothermal system (see text). Natural heat flux by fumaroles is calculated based on the distribution of underground temperature at 50 cm deep and its relationship with observed heat flux (Sugiyama et al. 1985); 7.4 W/m^2 (> 30 °C), 13.4 W/m^2 (> 50 °C), 21.5 W/m^2 (> 70 °C), 29.0 W/m^2 (> 85 °C) and 837 W/m^2 (> 90 °C). The latest distribution of underground temperature appears in Fig. 15

Table 1 Maximum temperature of fumarole steam at Owakudani from the historical literature (after Mannen 2009)

Year	Observer	Max. temperature (°C)
1872	J. P. I. Vidal	103
1917	F. Omori	141
1920	T. Kato	106
1921	T. Kato	97
1925	S. Tokuda	98
1932–1933	M. Sugiyama and O. Okada	102
1951–1953	I. Iwasaki	86
1966–1967	K. Yuhara	138 (steam well?)

In 2013, the heat flux of Owakudani showed a sharp drop of up to 6 MW (Fig. 3a) and the ratio between NHF and SPW flux diverted from a line formed by previous observations (Fig. 3b). In the summer of 2011, a new steaming area named Region E was formed north of Owakudani (Fig. 2; Harada et al. 2012). The heat flux of Region E was estimated to be 7–8 MW in 2013 and 2014, and this is almost the same as the 2013 heat flux drop at Owakudani. The sharp drop at Owakudani can thus be explained by the bypassing of deep geothermal water to Region E.

Controlled Source Audio-frequency Magneto-Telluric (CSAMT) analysis carried out in 2014 seems to support this hypothesis (Fig. 4). The geothermal fluid represented by low resistivity seems to be supplied from the north to the Owakudani area; however, a bypass route appeared to connect the main stream of geothermal fluid and the ground surface of Region E. This bypass route could have been formed by the strong ground motions caused by the 2011 Tohoku earthquake and induced earthquakes at Hakone (Yukutake et al. 2011a), although no surface deformation was observed after the seismic event.

The 2001 unrest

Prior to the 2015 eruption, the 2001 unrest was the most intense since continuous volcano monitoring began in 1959. This unrest was characterized by a significant rise of geothermal activity as inferred from blowout of SPWs and ground deformation detected by tiltmeter and the GNSS network; earthquake activity was the highest

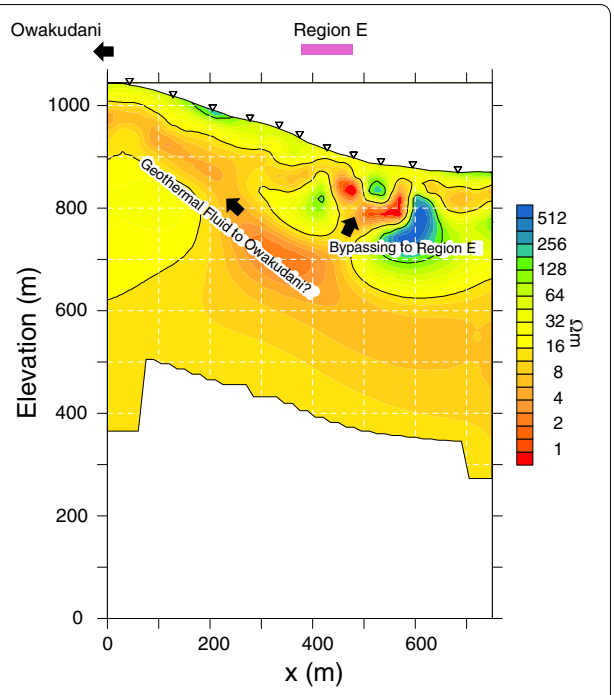

Fig. 4 Cross-sectional structure of resistivity of north Owakudani through Region E observed in 2014. The surface projection of the cross section is shown as Section K in Fig. 2 (Courtesy of Waterworks Department, Public Enterprise Agency of Kanagawa Prefecture)

recoded to date in terms of magnitude and duration (Harada et al. 2013). Although this event did not culminate in an eruption, its sequence was similar to that of the 2015 eruption discussed later.

According to Daita et al. (2009), the 2001 unrest began with slight tilting starting on May 23, 2001. It was followed by sudden temperature rises (up to 5 °C) at a few hot springs in Gora (Mannen 2008). This increase started on May 28 and continued for a few days, with high-temperature status remaining until mid-September. On June 12, seismicity increased dramatically and peaked around early July (Fig. 5c). With seismic activity, the tilt rate increased drastically and continued until early September (Daita et al. 2009).

The largest earthquake ($M = 2.9$) occurred at 11:40 on July 21 (Japan Standard Time in this paper; JST = UTC + 9). A few hours after the earthquake, one of the SPWs named no. 52 (500 m in depth) started to emit significant amounts of steam and became uncontrollable. Normally, the SPWs in Owakudani are controlled by water injection to the mixing facilities above the well mouth. The blowout condition is thus defined as a status in which available water and the mixing facility are not enough to condensate the steam. At the same time, steam from SPW no. 39 (413 m deep) intensified to nearly blowout condition and proximal hot springs shown in Fig. 2 began steaming vigorously (Tsujiuchi et al. 2003). From SPW no. 52, volcanic gases such as H_2S, SO_2 and HCl were released and the steam temperature, measured on September 21, 2001, was 163.3 °C (Ohba et al. 2008). On July 22, four deep low-frequency events (DLFs), which is considered to indicate migration of magma or magmatic fluid, were observed.

Tilt change during the event is interpreted as inflations of a single Mogi source located about 7.0 km deep near Komagatake and the opening of two cracks near Owakudani and Komagatake (Fig. 1b). Inflated volumes were calculated to be 7.1×10^6, 0.15×10^6 and 0.51×10^6 m^3, respectively (Daita et al. 2009). Based on seismic tomography, causes of these inflations were considered to be magma for the deep Mogi source and geothermal fluid for the shallow open cracks (Yukutake et al. 2015).

After the 2001 unrest, smaller volcanic unrests took place in 2006, 2008–2009 and 2013. No steaming anomalies were visible during these events; however, the composition of gases, such as the carbon-to-sulfur ratio (hereafter C/S ratio), showed sharp increases when the unrests began and gradual decay as the unrests diminished (Ohba et al. 2008).

Chronology of the 2015 eruption

Precursor (early April–June 2015)

The 2015 eruption of Hakone volcano occurred on June 29, 2015; however, its precursory unrest started as a slight inflation of the deep Mogi source from early April (Fig. 5a). It is noteworthy that an unprecedented swarm of DLF was observed on April 5; according to the JMA unified catalog, 16 DLFs were recorded on the day (Fig. 5c).

Deep inflation was recognized until the end of April and the earthquake swarm started on April 26. After this time, seismicity increased rapidly and reached its climax on May 15, when 955 earthquakes ($M \geq 0$) were observed (Fig. 5d). Then, seismicity gradually decreased, although the daily number of earthquakes highly fluctuated.

The epicenters of the earthquake swarm were mainly located on a zone traversing the post-caldera central cones from north to south (Fig. 6). This zone was seismically active through the duration of the earthquake swarm, although there were several surges of seismicity, the duration of which were less than a day and more than tens of earthquakes occurred within a small region (~ 2 km in diameter). These seismic surges accompanied tilt change near the epicenter region (Fig. 7), and hypocenters, precisely determined using the double-difference (DD) method, showed platelike distributions (Fig. 6). Although detailed analysis of seismic surges during the 2015 unrest is yet to undertaken, these features seem to imply fluid injection as observed during the 2008–2009 unrest (Yukutake et al. 2011b).

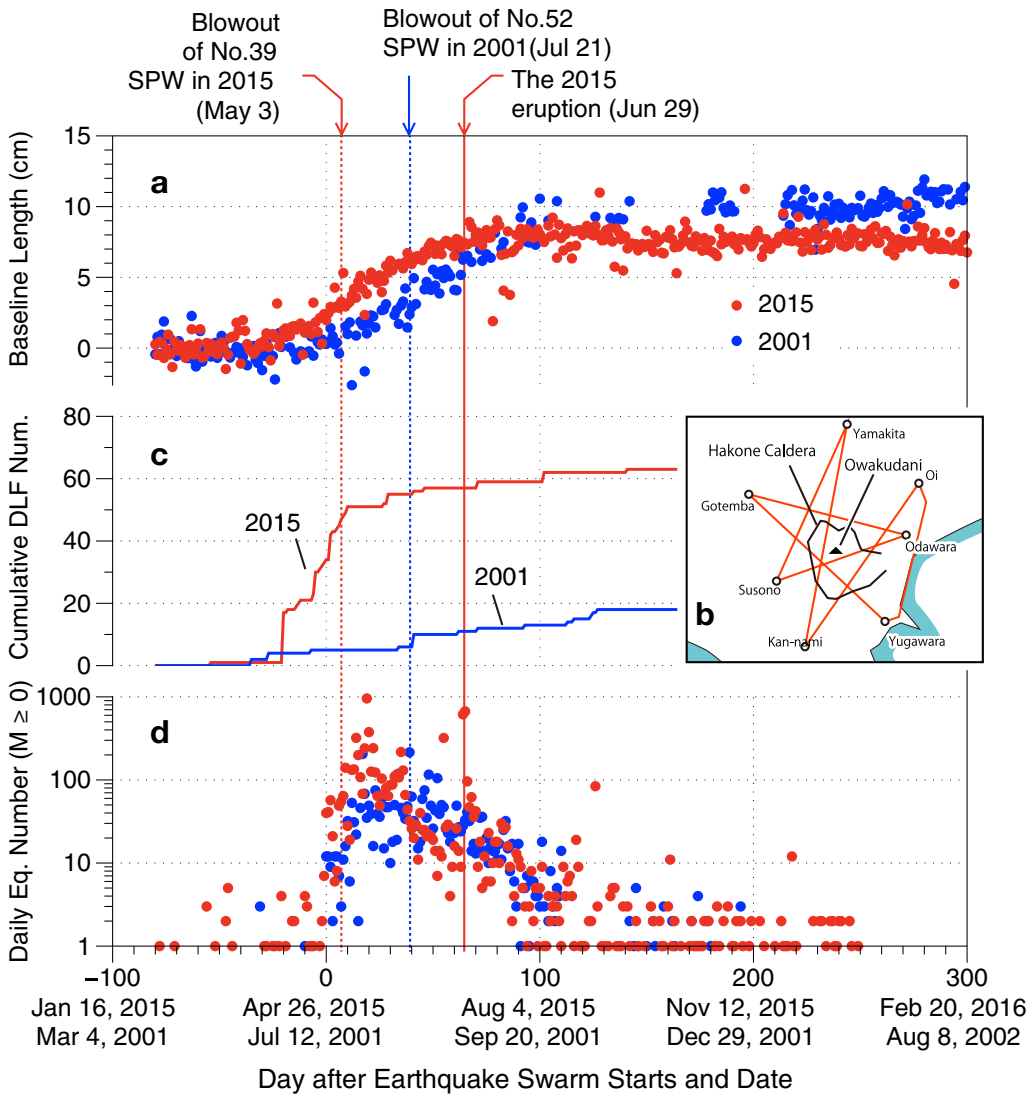

Fig. 5 Sequential changes of crustal inflation and seismic activity during the 2001 unrest and 2015 eruption (Harada et al. 2015). **a** Crustal inflation is represented by normalized baseline lengths across the volcano (the stacking method; Miyaoka et al. 2011; Miyaoka and Takagi 2016). The baselines used in **a** are shown in **b**. **c** Cumulative number of deep low-frequency event (DLF). **d** Seismic activity is represented by daily number of earthquakes at Hakone volcano ($M \geq 0$)

Anomalies of steam activity first manifested as intensified steaming of no. 39 SPW at Owakudani on April 16 (Fig. 8a). Since no. 39 SPW had been less productive, this intensification initially pleased the hot springs company; however, in the early morning of May 3, the well fell into a blowout condition (Fig. 8b). The usual hot spring production of no. 39 SPW was 50 m^3/day, but after this time, available water of 500 m^3/day was all blown away by intensified steam gushing out from the top of the mixing facility. On May 7, InSAR analysis detected a slight and very local uplift (up to 7 cm within an area of < 100 m radius) around no. 39 SPW (Doke et al. 2018; Kobayashi et al. 2018). After mid-May, steaming activity started from the ground surface around no. 39 SPW (Fig. 8c) and gradually intensified. In contrast, steaming activity of no. 39 SPW diminished and stopped by late June (Fig. 8d). Also, formations of open cracks were recognized on the ground surface around the well in June (Fig. 9). Due to the steaming activity around the SPW, the ground surface was rarely observed in late June.

Eruption (June 29–July 1)

Ashfall

The weather during the eruption duration did not allow us to make a continuous visual observation. On June 29 and 30, it was generally cloudy and the Owakudani area

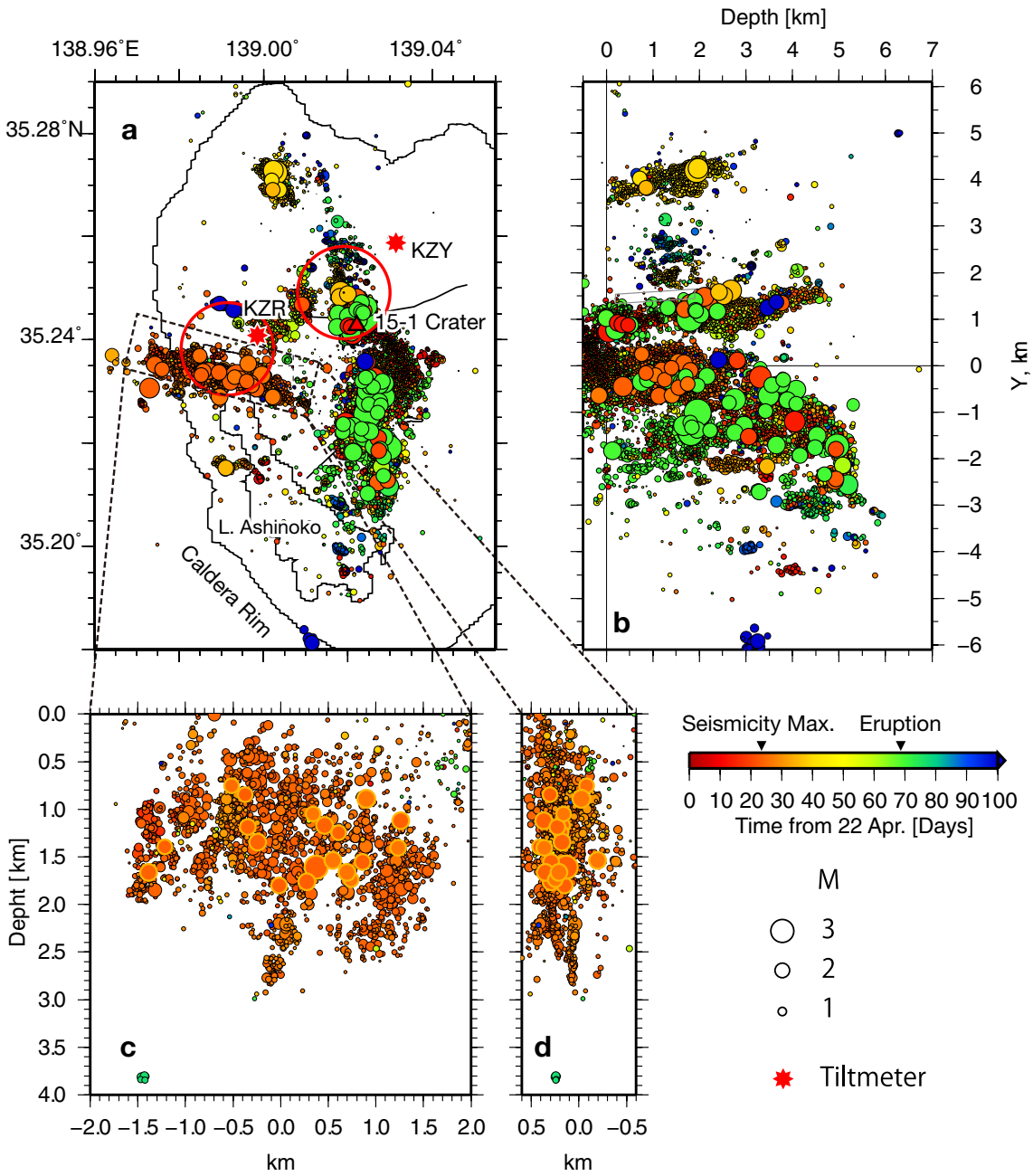

Fig. 6 **a** Epicenter distribution during the 2015 unrest and eruption of Hakone volcano (from April 22 to July 31). **b** Depth distribution of **a**. Seismicity seems to concentrate along planes likely formed by open cracks; an example in the Kojiri area is shown by depth distributions along strike (**c**) and dip (**d**) directions. Temporal seismicity change within the red circles during the unrest is shown in Fig. 7

was covered by fog, although sky cleared up temporary in the early morning of the 30th. During the daytime of these days, there was no rain except for a weak shower (1 mm at the Hakone automated weather station 3 km SE of Owakudani) in the early morning (5–7 am) of the 29th. Generally, wind was mild on 29 and 30 of June. On July 1, however, it was windy and rained heavily (maximum hourly rainfall of 20.5 mm at the automated station) until the evening due to the passage of a typhoon.

After mid-May and before the day of the eruption, the seismic activity of Hakone volcano decreased slowly (Fig. 5d) and then suddenly increased from 7:32 on June 29. However, visual observation was next to impossible for that day until late evening due to fog.

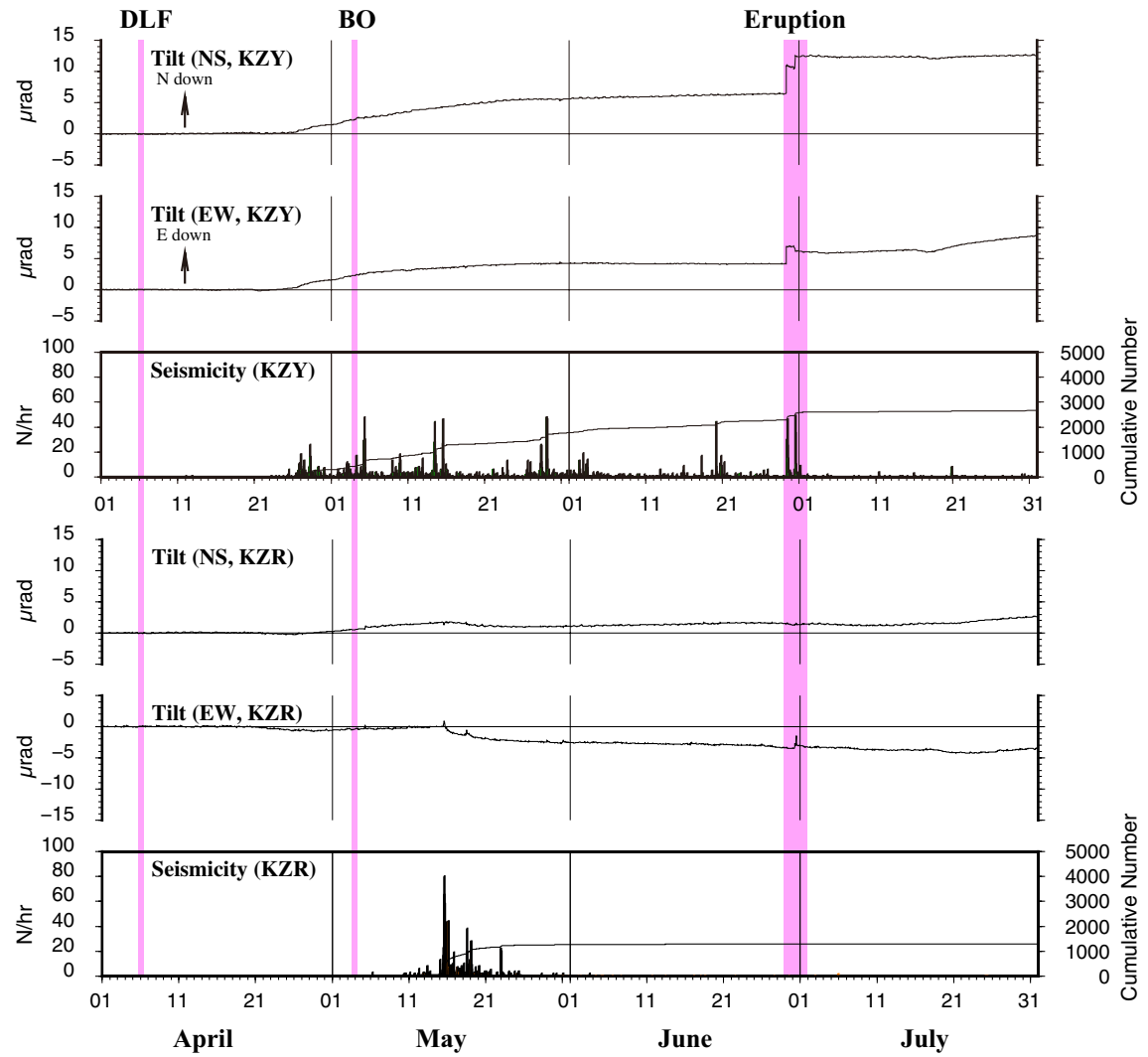

Fig. 7 Tilt changes (NS and EW components) and seismicity from tiltmeters in Kozukayama (KZY) and Kojiri (KZR). Timings of the initial swarm of the deep low-frequency event (DLF), blowout of the No. 39 SPW (BO) and the eruption are also shown. Seismicity here indicates hourly number of earthquakes within circles shown in Fig. 6. In KZY, seismicity and tilt change are evident in late-April to mid-May and on eruption days. In KZR, both increase in mid-May

The eruption was recognized first by ash fall, described as "mud rain," by a mobile observation team of JMA (MOT-JMA) at Sounzan station and inhabitants in the Gora area (Fig. 1), approximately 1 km east of the eruption center, at around 12:45 on June 29 (Fig. 10a). A time-lapse camera installed at Owakudani did not take images of the ground surface due to fog at that time; however, it captured a sudden and transient fall of droplets on the camera window at approximately 12:30 (Fig. 11). Since the droplets left grime on the window (Fig. 11d), the droplets are considered to have been the mud rain observed in the Gora area. No more ash or droplets were observed by the time-lapse camera after that time. However, ash fall was observed by residents in areas around Owakudani, such as Gora and Sengokubara, until June 30, with the total erupted ash volume estimated at $0.8–1.3 \times 10^5$ kg (Furukawa et al. 2015). In the early phase of the eruption, the ash fall took the form of wet mud rain and adhered to the surface on which it landed (Fig. 18a, b); however, in the later stage, the ash became drier, which allowed easy sampling.

On the surface of a GNSS instrument (REGMOS) installed by the Geospatial Information Authority of Japan (Fig. 2), ash fall tracks were recorded as grime formed by droplets of mud or mud rain (Fig. 10b). The track direction implies that the droplets came from the

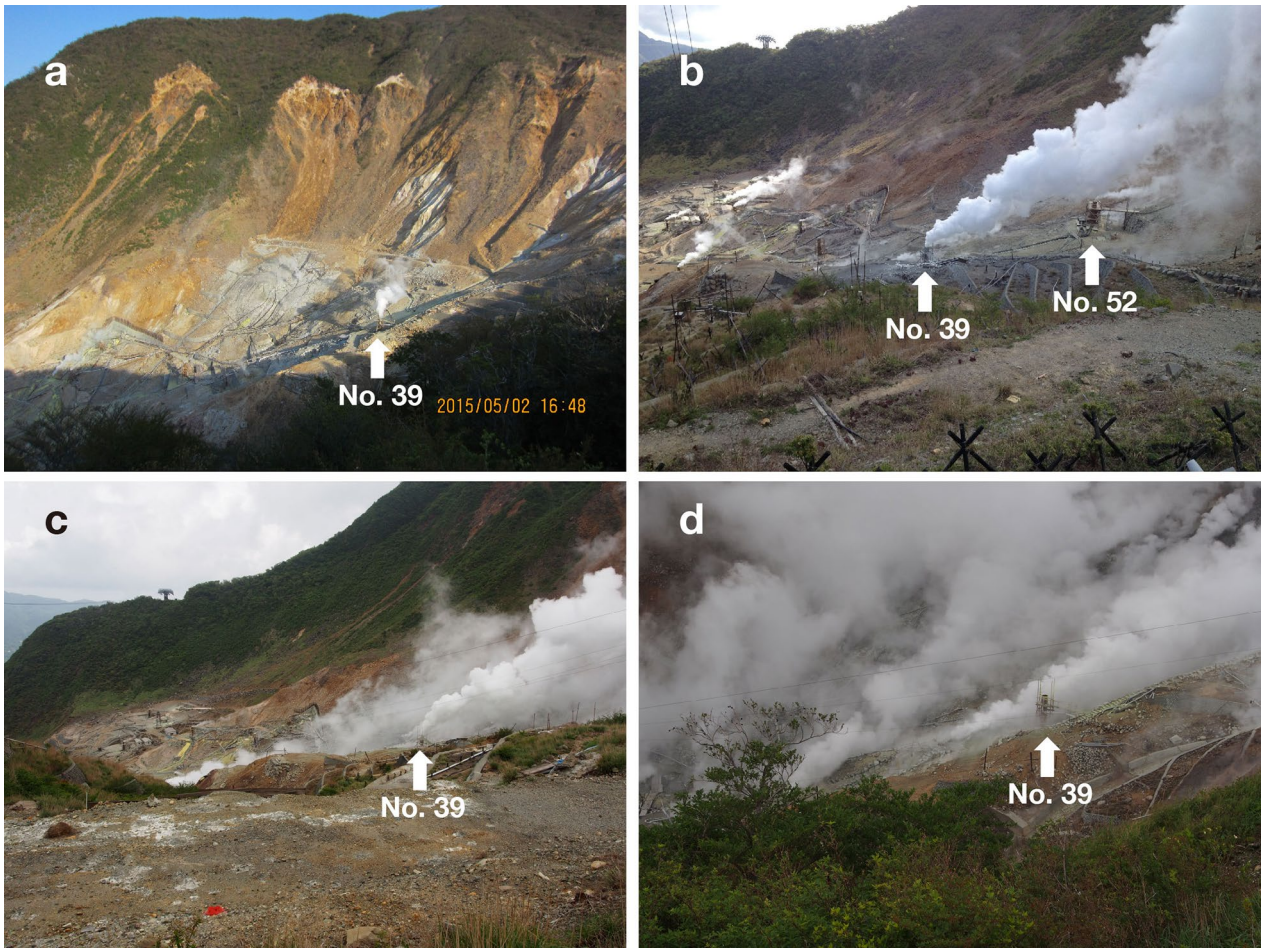

Fig. 8 Development of steaming activity at Owakudani before the 2015 Hakone eruption. See Fig. 2 for the shooting locations. **a** Slightly intensified steaming from the no. 39 SPW (16:48, May 2, 2015; from location **c**. **b** Blowout of no. 39 (7:36, May 3, 2015; from near REGMOS). **c** Ground steaming around the no. 39 SPW (10:35, May 18, 2015; from near REGMOS). **d** Ground steaming around the no. 39 SPW (9:04, June 20, 2015; from near HSRI camera). Note that no. 39 SPW is not steaming in late June. All photos were taken by HSRI

vent area. From the tracks, the average droplet diameter is estimated to have been approximately 2 mm. Since the fall velocity of a droplet of this size is estimated to be approximately 7 m/s (Beard 1977) and the angle between the ash fall tracks and the vertical line was approximately 60°, the wind velocity is estimated to have been 12 m/s ($=7\times\tan 60°$). We observed no such wind gusts during our stay in the area from 1 h later than this time. Based on this observation, we suspect that the vent proximal area may have been covered by a very dilute base surge, which contained droplets of mud. This is also implied by the sudden droplet fall on the time-lapse camera installed northwest of the vent area, while wind was generally blowing from the north on June 29.

The eruption plume that caused the ash fall was not observed well due to fog and cloud that covered the vent area; however, several shots, taken by a live camera installed by JMA at Miyagino, in the early morning of June 30, are the exception and a plume rising more than 2.8 km above sea level (1.8 km above vent) can be recognized (Fig. 10c).

Mud flow and debris flow from the vent area

Soon after the recognition of ash fall, scientists of Hot Springs Research Institute of Kanagawa Prefecture (HSRI) formed a joint team with MOT-JMA to investigate the eruption center and discovered a mud flow going down the main stream of the Owakuzawa River in the bottom of Owakudani valley (Fig. 12a). The mud flow was colored gray and appeared to be slurry containing large amount of clay. Although the mud flow carried logs and lumbers, which had been parts of simple handmade bridges over the streams installed by the hot spring company, no blocks and boulders were observed within

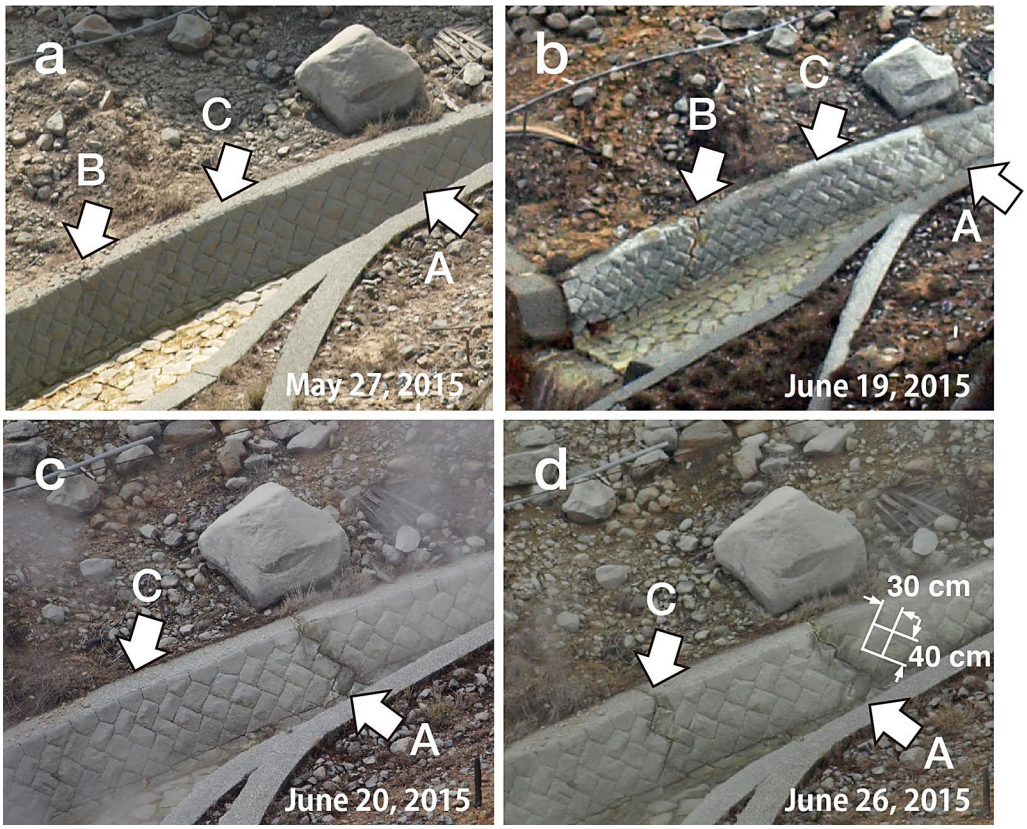

Fig. 9 Cracks appeared on a training wall near the no. 39 SPW in Owakudani. White arrows indicate the positions where cracks were formed. **a** On May 27, no apparent cracks had formed. **b** Three weeks later, cracks A and B with sulfur and ferrioxide at the opening had formed. **c** From crack A, water seems to be seeping out but the place where crack C will be formed seems intact. **d** A week later, crack C is newly formed. The size of the stone blocks paving the wall is 40 cm × 30 cm. The location of these cracks is shown in Fig. 2. All photographs are taken by HSRI

the flow. The mud flow was small enough to be almost confined within the training wall installed at the bottom of the valley. The average volume flux of the flow is estimated to have been approximately 1 m^3/s from the geometry of the training wall and flow velocity, although the flow rate changed significantly during our observations. Such fluctuation of the flow rate was also inferred from the mud flow deposit downstream (Fig. 12b).

The flow rate of the mud flow was significantly higher than the production rate of artificial hot spring in the valley (< 0.06 m^3/s). The high flow rate of the mud flow thus cannot be attributed to the rupture of plumbing systems of artificial hot springs in the upper stream. Since no heavy rainfall was observed before or during the eruption, and the usual flow rate of the stream (~ 0.1 m^3/s) is much lower than the flow rate of the mud flow, the mud flow seems to have been derived by the eruption directly from the vent.

After the eruption, we identified a tributary in which gray colored water was flowing even at the time of investigation on July 10 (Fig. 12d), while water in other tributaries remained clear. Here we call the affected tributary Stream L. The source vent of the mud flow is expected to have formed in the upstream area of Stream L.

Separate from the mud flow, a debris flow deposit was recognized within the vent area in a photograph taken at 17:29 on June 29 (Fig. 12c). After the eruption, we found the debris flow deposit to be composed of coarser material such as andesite blocks, breccias and sands, which are common to surface material of the steaming area and travelled down to near SPW no. 55 along Stream L (Fig. 12d). The debris flow is thus considered to have also flowed down Stream L.

The area of the 2015 eruption center is a location for hot spring production and comprises a complex pipeline system. Among the pipeline system, the largest water pipe crossing under Stream L was found eroded and ruptured after the eruption. Since a temporary but significant decrease in artificial hot spring water coming down from the production area was observed by workers of the hot spring company at around 11:00 on June 29, it is reasonable to assume that the mud flow and/or debris

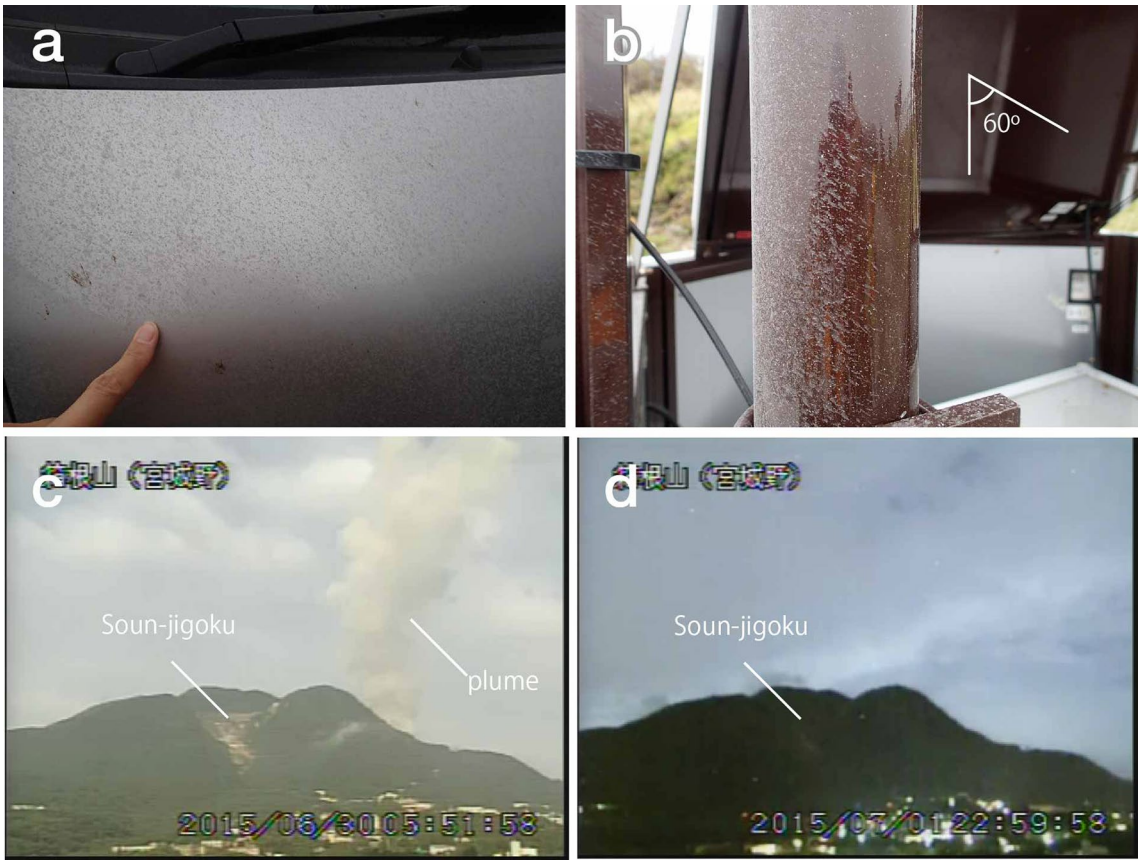

Fig. 10 Photographs taken during and after the eruption. **a** Ash fall on the bonnet of a car at Sounzan station (Fig. 1; 13:52 of June 29). **b** Ash fall on a REGMOS at Owakudani (Fig. 2; 14:40 of June 29). Note that the ash fall track is inclined. **c** Plume of the 2015 eruption from Miyagino, east–northeast of Owakudani at 5:51 of June 30. **d** Photograph taken from Miyagino at about 23:00 on July 1 shows no apparent plume above the eruption center. Photographs were taken by HSRI (**a**, **b**) and JMA (**c**, **d**). See Fig. 1 for location of the JMA live camera

flow eroded Stream L to decrease the water supply at this time. Since the hot spring water coming down from the area completely halted until 15:00, the water pipe seems to have been broken until this time. We thus conclude that some liquid effusion process started before 11:00 and eroded the streambed significantly until 15:00.

Source vents

On June 29, the steaming area was covered by fog and erupted steam. Although we were able to take a brief look at a crater emitting steam vigorously at 16:37, we could not confirm the observation satisfactory during our stay in the vent proximal area which lasted until 18:30. However, in the late evening, cameras occasionally captured vigorous eruption plumes rising from several sources (Fig. 13b).

On June 30, slightly better weather and less intense steaming enabled us to take a glance at the ground surface of the eruption center and we observed a newly formed crater, the diameter of which was estimated to be approximately 7 m (Fig. 14a). From the crater, an eruption column was formed and blocks up to 30 cm in diameter were thrown occasionally reaching up to 20 m high above the crater.

In this study, the source vents which formed small cones are defined as craters and other sources of steam are termed newly formed fumaroles (NFF). After the eruption, we mapped the locations of craters and NFF in the steaming area and assigned identification numbers (Fig. 15). The numbers were assigned in the order of discovery without distinction of types. The initial 15 before a hyphen refers to vents formed in 2015, and this nomenclature is a directive of JMA.

Timing of NFF formation was not monitored well due to fog and steam, although those nearest to the lookout platforms seemed to be active from the first scene taken by the time-lapse camera and remain active at the time of writing. On the other hand, images taken by the time-lapse camera revealed that craters had a more complex history of formation and extinction.

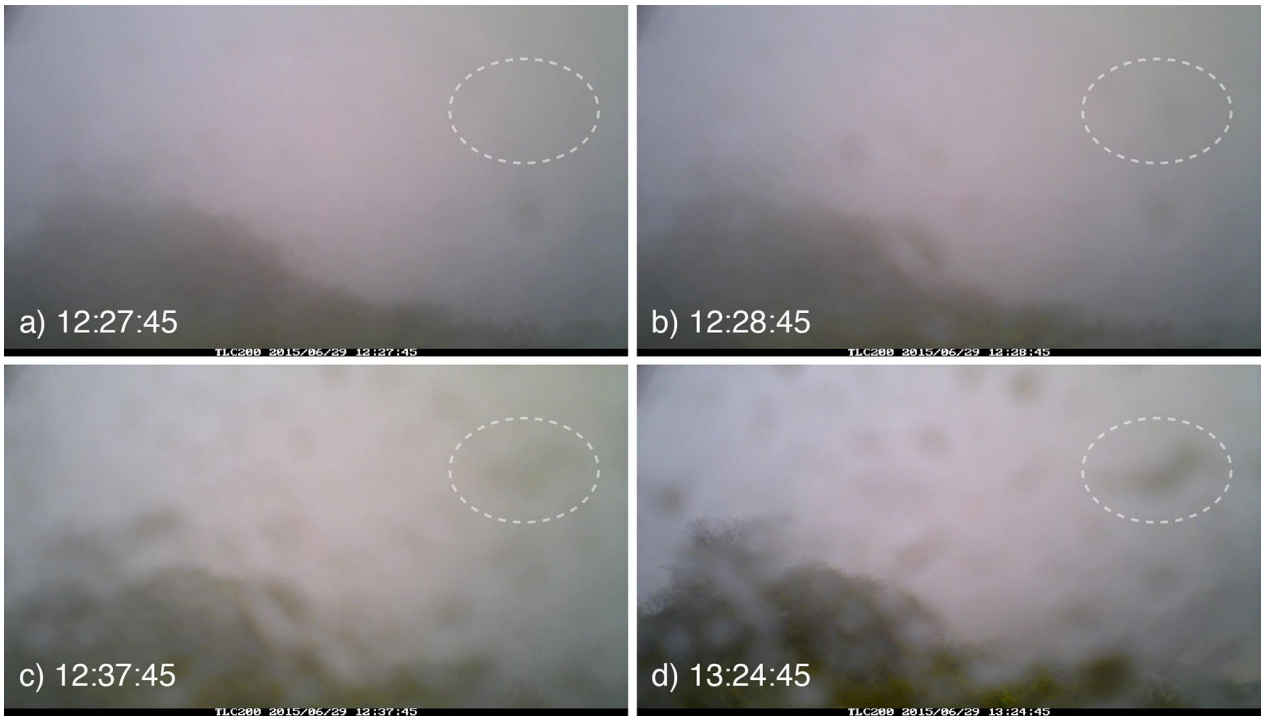

Fig. 11 Images taken by a time-lapse camera at around the time when ash fall was first observed on June 29, 2015. **a** The area of eruption was covered by dense fog but no rain fall was recognizable until 12:27. **b** Rain fall began at 12:28 and **c** covered whole camera view until 12:37. **d** The window surface began to dry; however, grime remained (13:24). The oval shows a reference area where a rain drop fell at 12:37 and remained as grime after the water evaporated. The camera was installed by HSRI (Fig. 2)

The craters formed first were 15-9 (Fig. 13b) and 15-6 (Fig. 13c). Since these craters were formed in the uppermost part of the Stream L, it is reasonable to assume that the mud flow and debris flow originated from the craters. They seemed to be active until at least the early morning (4:49) of June 30; however, they were found to be extinct at 8:22 of the same day, and at that time, the newly formed 15-5 was found active (Fig. 13e). The cones formed around 15-6 and 15-9 were found eroded on the morning of July 1, and after the eruption, only weak fumaroles were recognized at these sites.

The 15-5 crater had remained active until early morning of June 1; however, when 15-1 was found active at 4:46, the 15-5 crater was found extinct. The 15-1 crater, the rim to rim diameter of which is approximately 15 m, is the largest crater formed during the 2015 eruption. It is noteworthy that the location where craters formed did not show any signs of geothermal activity (Fig. 15) or ground deformation before their formation.

Ballistic clasts

Fortunately, the range of ballistic clasts from the 2015 Hakone eruption was very limited. We witnessed ballistic clasts flying from the 15-5 crater on the morning of June 30 (Fig. 14a). At that time, the crater was active and the ballistic clasts seemed to land barely 15 m beyond the crater rim. On the other hand, several large rocks (~30 cm in diameter) were found after the eruption on a trail approximately 30 m from the crater rim (Fig. 14b). However, the clasts did not seem to accompany any apparent impact crater near to them as we observed from a distance. Thus, the large rocks could have fallen from the slope, although originally expelled from the vent and landing on the slope near the crater. Here we define the bombardment range as less than 30 m.

Seismicity

Seismic activity surged after 7:32 on June 29, mainly composed of high-frequency earthquakes. Interestingly, the high-frequency activity started from shallow (< 1 km below sea level) and gradually propagated deeper (5 km below sea level) in the first approximately 24 h (Fig. 16). Intense earthquakes took place when the propagation ended and this seems to have been coincident to the new vent formation (15-5) in the morning (4–8 a.m.) of June 30. The largest earthquake during the 2015 unrest and eruption occurred at this occasion (6:56, $M = 3.4$).

Fig. 12 Photographs of mud and debris flows. See Fig. 2 for shooting locations. **a** Lahar flowing down Stream L in Owakudani (15:56 of June 29). **b** A flow channel downstream of **a**. Note that mud deposits are wider than that of the stream width at that time, which implies a higher flux of mud flow in the early phase of the eruption (15:09 of June 29). **c** Eruption center during the eruption (17:29 of June 29). Debris flow deposit had been emplaced. **d** Debris flow deposits near no. 55 SPW (9:10 of July 10). Note that the stream across the debris flow deposit (Stream L) is colored gray, even 9 days after the eruption. Large rocks on the left bank and right of the scale were set before eruption by the company to protect no. 55 SPW. All photographs were taken by HSRI

Concurrent to the surge of high-frequency events, a rapid tilt change (RTC), which was the first observed at the volcano, took place and several similar events followed until 13:00. RTC is defined as a tilt change in which the duration is short (~ 150 s) and seems to have been generated by crack formation that fed hydrothermal fluid to the surface (Honda et al. 2015). After initiation of the eruption, harmonic tremors and infrasonic waves, also the first observed at Hakone volcano, occurred and are interpreted as boiling and surfacing of thermal fluid (Yukutake et al. 2017, 2018).

Termination

Generally, it is difficult to identify the end of an eruption. This is especially the case for the 2015 eruption as ash dispersal was limited and visual observation of the vent area was inhibited due to bad weather and intensive steaming. Ash fall in inhabited areas was recognized until the morning of June 30 (Furukawa et al. 2015); however, a new crater (15-1) was formed in the early morning of July 1, and this event seems to have accompanied the most intense harmonic tremor and infrasound in the eruption sequence (Yukutake et al. 2017, 2018). We thus conclude that large amount of energy had been released in the early morning of July 1. Since a typhoon was passing during the daytime of July 1, we did not enter the Owakudani area. The cameras also failed to take images of the eruption center due to the poor visibility. After the passage of the typhoon in the late night of July 1, no eruption plume was visible (Fig. 10d). This observation indicates that steam from the crater became sufficiently weak to rise in moderately windy conditions. We thus consider that the eruption terminated at some time during the day of July 1. Since the tremor and infrasound seemed to have halted at about 7:00 on July 1 (Yukutake et al. 2017, 2018), the eruption may have terminated at this time.

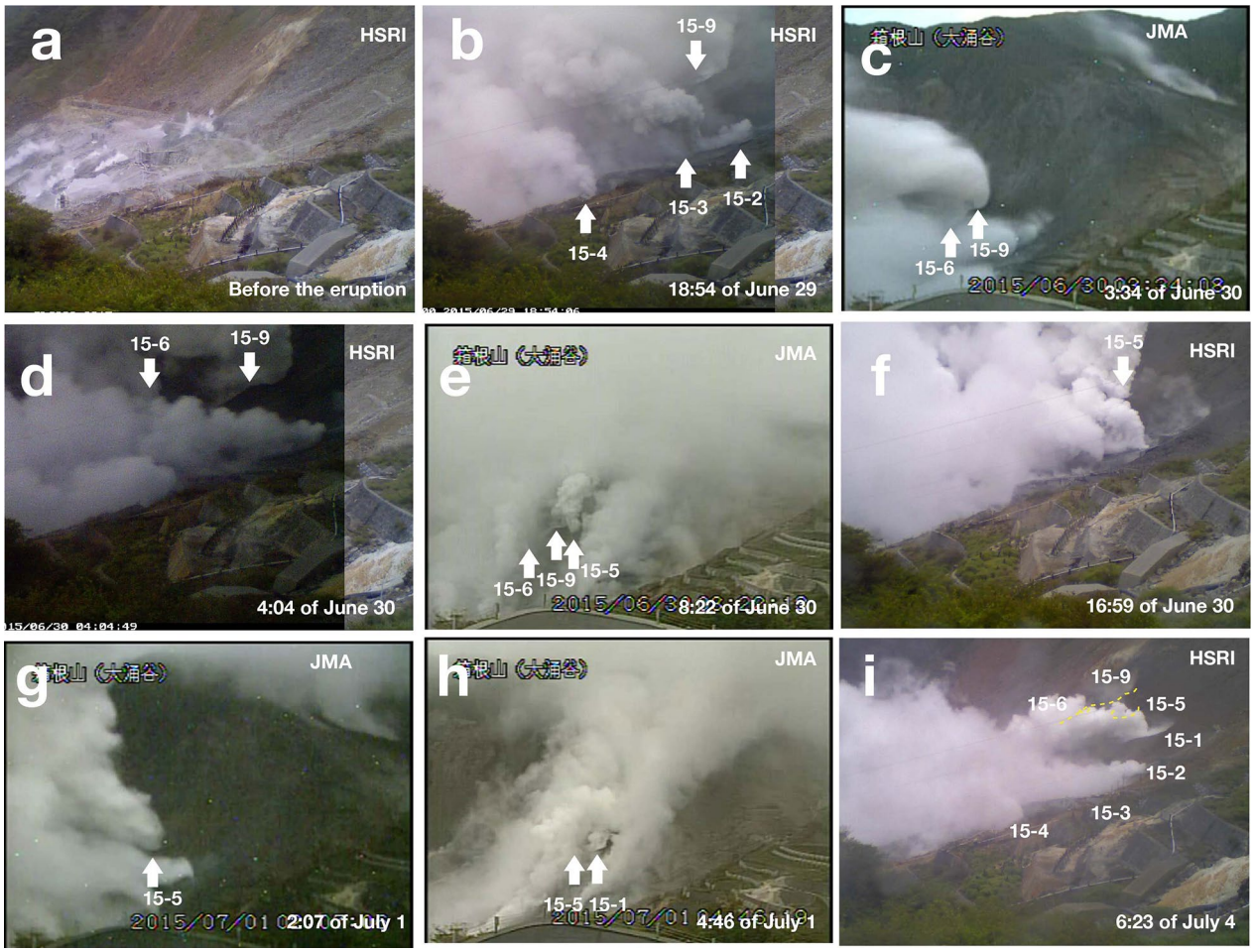

Fig. 13 Images of the eruption center and migration of the active crater during the 2015 eruption. Photographs were taken by a time-lapse camera (HSRI) and webcam (JMA). Locations of the cameras are shown in Fig. 2. **a** Area just before the 2015 eruption (darkened blending of images to erase steam). **b** First shot of active crater. A large crater (15-9) and intensive fumaroles (15-2, 15-3 and 15-4) are identified. **c** 15-6 and 15-9 seem to be connecting. **d** 15-6 crater itself was not observed from observation points; however, intensive steam in the photograph and geomorphological analysis after the eruption infers its existence. **e** The first shot of 15-5. Although 15-9 appears to be still active, the newly formed 15-5 seems more vigorous. 15-6 seems inactive. **f** It is evident that 15-5 had formed before 15-9 (c.f. photograph **b**). **g** The last shot of active 15-5. **h** The first shot of 15-1. The activity of 15-5 is not evident. **i** The first clear photograph taken after the eruption. Locations of extinct craters (15-5, 15-6 and 15-9) are also shown

Steaming activity after the eruption

After the eruption, steam emissions have vigorously continued to the present (early 2018). Among them, steam emissions from the 15-1 crater have been the largest and most vigorous since the eruption.

In the 15-1 crater, a boiling mud pool has appeared since July 3, 2015, when mud fountains higher than the crater rim were first observed from the ground (Fig. 17a). The mud pool suddenly exploded at 12:01 on July 21, and a jet of mud was thrown up to 46 m above the crater rim; however, almost all the material ejected went back into the crater and no significant ash falls took place beyond the crater rim (Fig. 17b). This event has accompanied no significant tilt, tremor or infrasound signals. It is difficult to say when the mud fountaining ceased, although it was not witnessed after November 2015. The mud water was monitored from March 2016 until it dried up in mid-August 2016 (Fig. 17c). The water was characterized by a very low pH and very high chloride and boron ions (Table 2). After drying up, the mud pool was filled by debris falling from a cliff behind the crater during typhoon rain on August 22. Following this, bubbling in the mud pool turned into several fumaroles, which are still vigorously emitting steam at temperatures above 150 °C at the time of writing (Fig. 17d).

The surface waters of Owakudani were also monitored before, during and after the eruption (Fig. 18). It is noteworthy that the level of Cl, which is considered a proxy

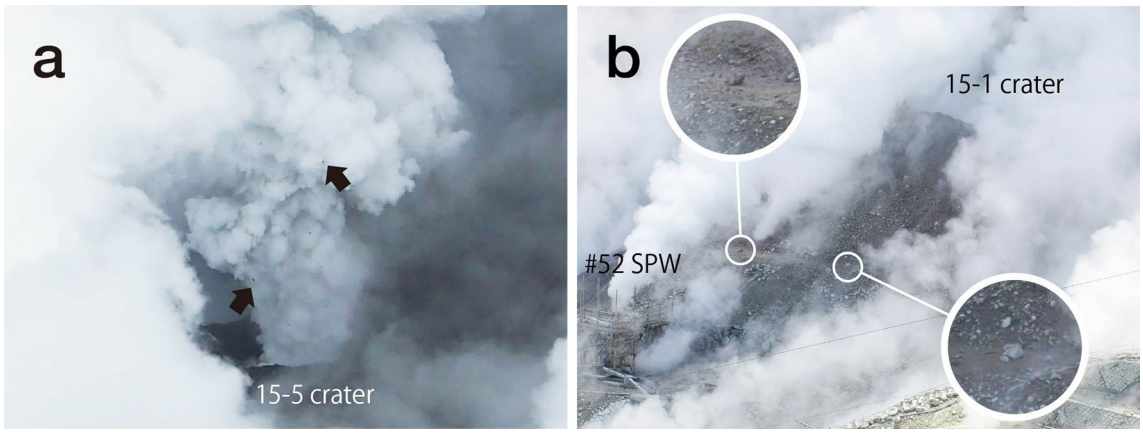

Fig. 14 **a** Ballistic clasts flying from the 15-5 crater. Arrows show examples of ballistic clasts. Diameter of the 15-5 crater was estimated to be 7 m (11:03 of June 30). **b** "Ballistic clasts" on a trail near the 15-1 crater (10:52 of July 10). All photographs were taken by HSRI from location c in Fig. 2

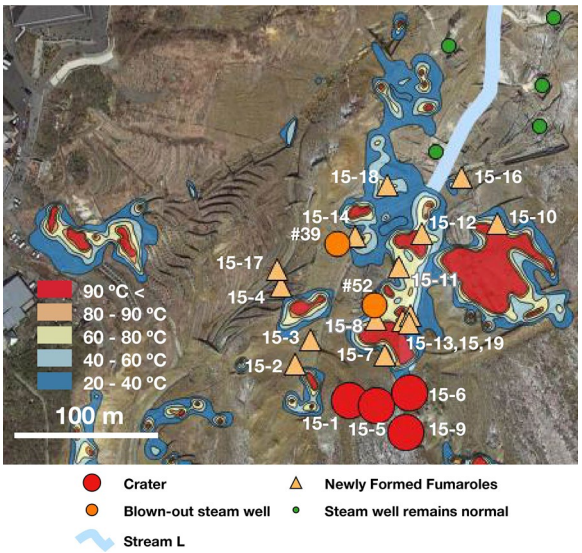

Fig. 15 Location of craters and fumaroles newly formed during the 2015 eruption (photograph source: Google Earth). Temperature distribution at 50 cm below the surface observed in February 2015 is also shown (courtesy of Odawara Public Works Center). Note that craters and many new fumaroles were formed where ground temperature was low before the eruption. Stream L runs through 15-12, 15-13 and originated from 15-6 and/or 15-9

of deep hydrothermal contribution, was not high when the volcano was erupting but became higher later. Downstream of the eruption center, high Cl was observed not at the time of eruption but soon after (early July to early August) and did not return to background levels until early autumn of 2016 (Fig. 18a, b). In the upper Owakudani area, the elevation of which (1066 m above sea level) is higher than the eruption center (1020 m asl), Cl content has been increasing gradually from after the eruption to the present (Fig. 18a, b).

Volcanic gas at Owakudani and surrounding areas has been monitored since 2001 (Ohba et al. 2008). Besides this, volcanic gas emitted from soil peripheral to the steaming area (Loc. 3 in Fig. 2) had been monitored using detector tubes almost bimonthly since October 2015. This gas shows that concentrations of CO_2 and H_2S, which are representative gas components of the region, are becoming gradually higher since the eruption, while CO_2/H_2S ratios are getting lower (Fig. 18c, d). However, in December 2015, a sudden increase in CO_2 and H_2S concentrations and CO_2/H_2S ratio was observed.

Photographs of the eruption center have been taken automatically by a time-lapse camera and a webcam installed by the HSRI and Industrial Research Institute (IRI) of Kanagawa Prefecture. Figure 18e shows average brightness of the eruption center area from the frames. The average brightness was high soon after the eruption; however, it came down to pre-eruption levels quickly. The average brightness increased again in late November 2015, peaking in mid-December, followed by a gradual decrease. This brightness increase is coincident with the sudden increase in volcanic gases mentioned previously. Since there is no measurement before December 2015, we are not able to see whether NFF temperature rose at this occasion. However, the NFF temperature seems to show a declining trend with some fluctuation (Fig. 18f).

Mitigation measures at Hakone volcano

Development of preparedness measures

Before the 2001 unrest, hazard mitigation plans for eruptions and unrest of Hakone volcano were virtually nonexistent. Consequently, no measures for public safety were conducted during the 2001 unrest, even though SO_2-rich mist gushing from SPWs had covered the sightseeing area of Owakudani. One reason for the omission

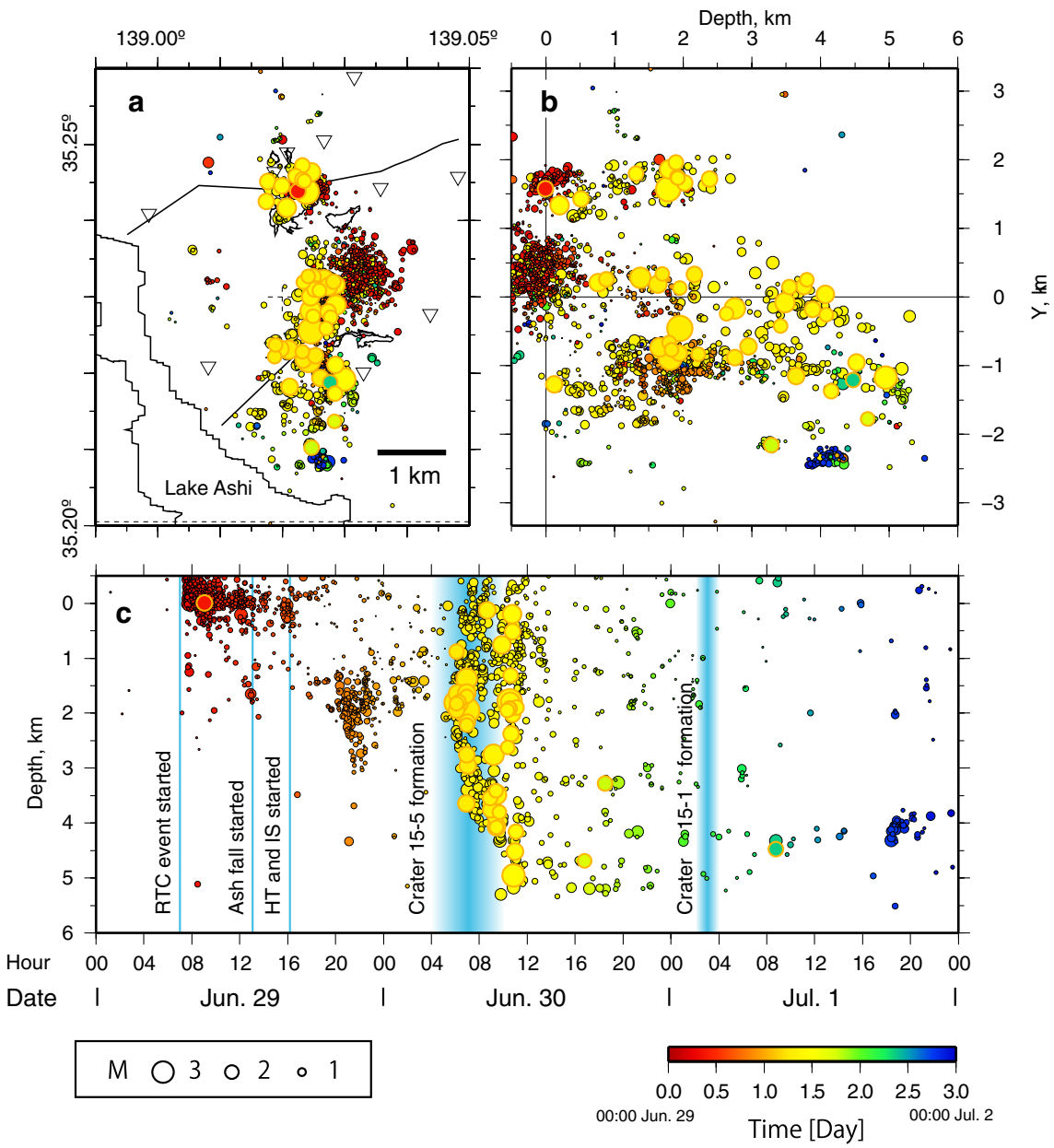

Fig. 16 Seismicity during days of the 2015 eruption (00:00 of June 29–00:00 of July 2). **a** Epicenter distribution. **b** Depth distribution along N–S cross section. **c** Time sequence of seismicity and another geophysical and visual observations. Beginning of rapid tilt change (RTC), ash fall, harmonic tremor (HT) and infrasound (IS) are shown. Timings of crater formations are also shown

was very complicated pluralistic governance of the Owakudani sightseeing area; the land owner was a private company, the trekking paths in and around the area were managed by the municipal government, the parking lot and road to the area were managed by the prefectural government, and the ropeway and bus to the area were run by two transportation companies. More importantly, there were no clear criteria to initiate evacuation from the sightseeing area. Although the law empowers mayors to declare evacuation instructions and to place areas off-limits, they need supportive criteria to demonstrate accountability for the declaration.

Since the 2001 unrest, the municipal government has begun to create a hazard map for volcanic activity. After a 2-year discussion involving a panel including academic experts, a hazard map was created and distributed to

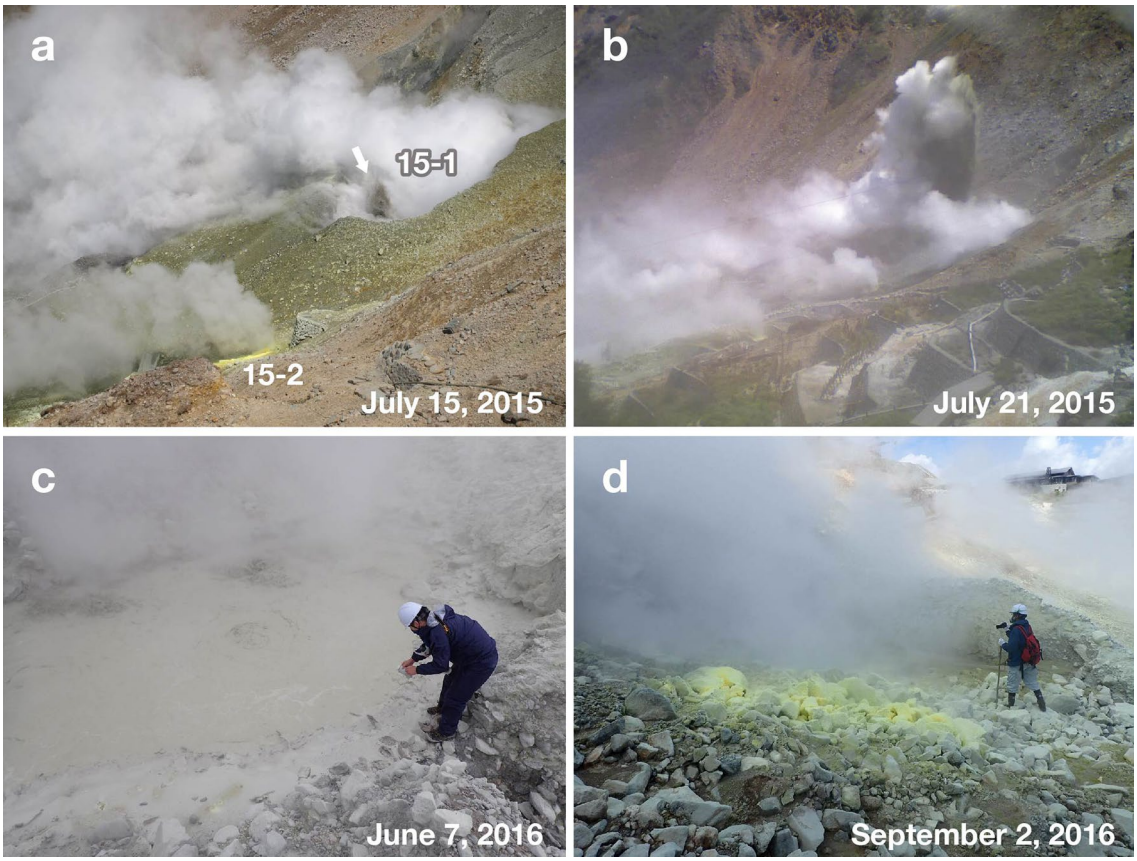

Fig. 17 Sequential change of 15-1 crater. **a** Soon after the eruption, a mud pool formed in the bottom of the crater and vigorous fountaining of mud (arrow) was observed. **b** A sudden and transient explosion at 15-1 crater on 12:01 of July 21, 2015. **c** Boiling mud pool formed within 15-1 crater. **d** Fumaroles formed after a landslide that took place in August 2016

Table 2 Chemical composition of mud pool water formed in the 15-1 crater

Date[a]	Temp (°C)	pH	EC[b]	Composition (mg/L)								
				Na	K	Mg	Ca	Fe	Al	Cl	SO_4	B
March 28	78.9	1.34	3.42	496	16.0	1210	1840	3500	2660	20,600	4700	220
May 13	93.1	1.76	2.02	139	12.6	178	384	3390	708	7180	1880	105
May 27	90.4	1.06	6.50	1060	156	1130	2490	4120	5740	38,400	3690	560
June 7	94.0	0.97	7.07	1120	138	1350	2650	3340	6060	39,100	3530	3030
June 27	94.6	0.79	7.05	74.1	21.7	220	225	2750	2630	20,500	1860	1670
July 14	94.4	0.05	37.4	206	54.4	636	478	5050	4770	65,300	2160	7620
July 28	95.2	< 0	> 20	439	134	744	970	2480	4580	87,600	3640	10,400

[a] Dates in 2016. [b]Electric conductivity (S/m)

the residents and business operators in the town in the spring of 2003. At that time, JMA was simply expected to describe the status of volcanic activity based on pure natural science; however, in 2008, the Meteorological Service Act was revised and JMA was obliged to announce volcano alert levels (VALs) when volcanic unrest or eruptions took place.

VALs are characterized by their linkage with mitigation measures implemented by municipal governments (Yamasato et al. 2013). Before the introduction of VALs for a certain volcano, JMA and municipal governments around the volcano must discuss and correlate mitigation measures and volcanic phenomena for each level.

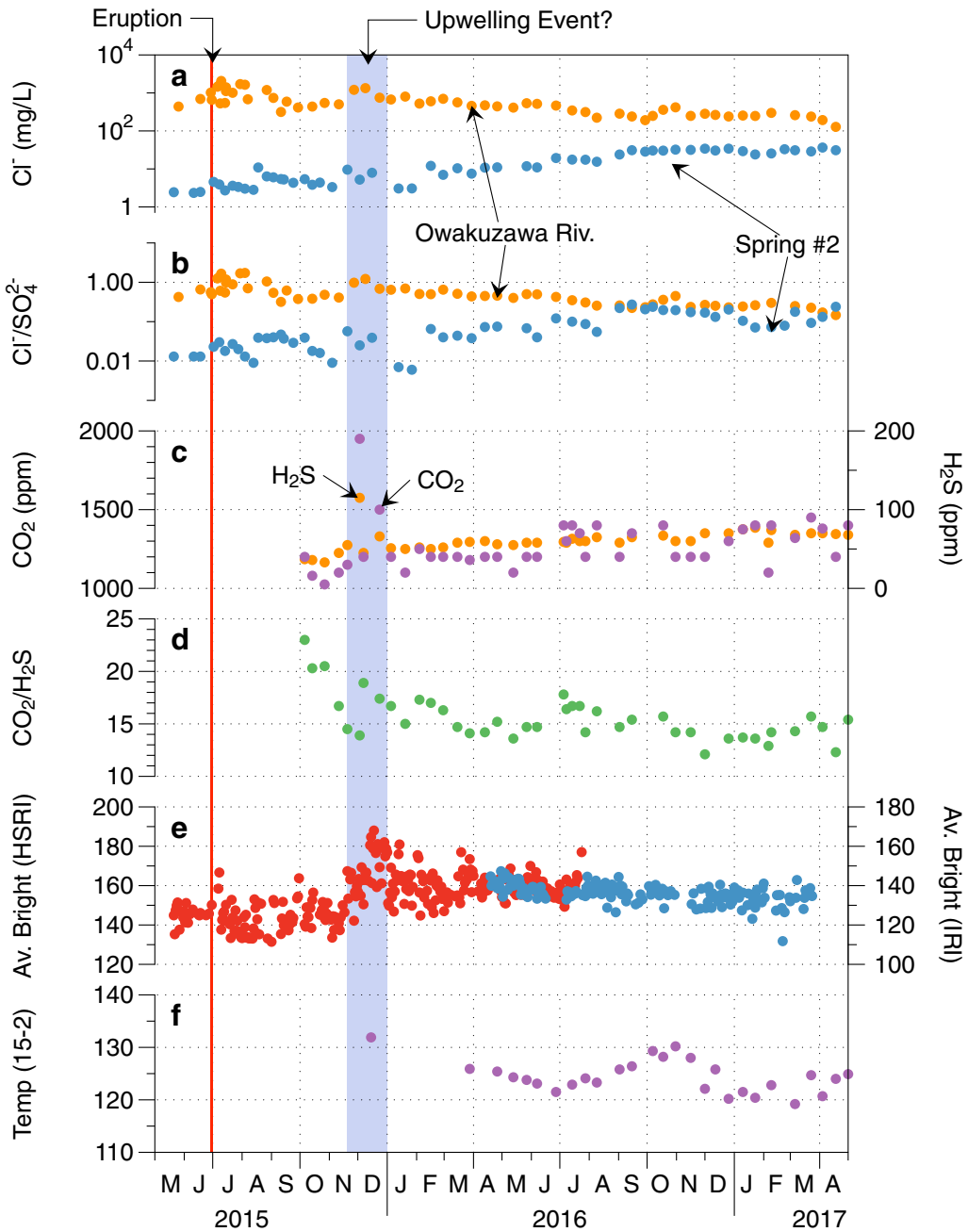

Fig. 18 Changes of water and gas chemistries, steam emission and temperature of steam from newly formed fumaroles at Owakudani before and after the eruption. **a** Cl^- content (ppm) and **b** Cl^-/SO_4^{2-} ratio of Owakuzawa River (Loc. 1) and natural spring #2 (Loc. 2). **c** CO_2 content (ppm) and **d** CO_2/H_2S ratio of volcanic gas seeping to the surface (Loc. 3). **e** Average brightness of digital images of eruption area. Since steam is white, average brightness of image of eruption area is expected to increase as a function of steam emission. Red dots imply value for images taken by time-lapse cameras installed by HSRI and blue dots for webcam installed by IRI. **f** Temperature of 15-2 fumarole. Sampling locations are shown in Fig. 2

For Hakone volcano, after a-year-long coordination processes among municipal and prefectural governments and JMA, VALs were introduced in March 2009. At the same time, the Disaster Prevention Council for Hakone volcano (hereafter DPC) was established. The task of the DPC is to make disaster mitigation plans and to give advice to the mayor.

VALs of Hakone volcano are based on a scenario, which traces the 2001 unrest and a possible phreatic eruption. In the scheme, it was decided to elevate VALs from 1

(normal) to 2 (do not approach the crater) when earthquake swarms, crustal inflation and steaming anomalies are observed at the same level of those observed during the 2001 unrest.

However, after the 2014 eruption of Ontake volcano, which resulted in fatalities even though the VAL remained at 1 (normal), the DPC for Hakone volcano established a manual that enables partial and full evacuations from the Owakudani sightseeing area even if observed unrest is subtler than that required to elevate to a VAL of 2. The manual went into effect on March 27, 2015.

Volcanic alert levels during the 2015 unrest

As mentioned, the 2015 volcanic unrest of Hakone was first recognized at the end of April and the earthquake swarm started on April 26. These observations were shared among members of DPC on April 28, when they assembled to attend the first evacuation drill carried out in the Owakudani sightseeing area after establishment of the evacuation manual.

The blowout of no. 39 SPW was recognized by a researcher of HSRI in the early morning of May 3 and it was immediately reported to the security and disaster management bureau of Kanagawa prefectural government, which is the secretariat of the DPC. The first meeting of the DPC was held on that afternoon, and it was decided to close trekking courses around Owakudani area from the next day. A DPC meeting was also held on May 5, and the procedure for total closure of Owakudani sightseeing area was discussed.

On May 5, larger earthquakes ($M > 2$) took place near Owakudani and, in the early morning of May 6, the VAL was elevated to 2 and the Owakudani sightseeing area was completely closed based on the procedure. At that time, the entrance of workers, researchers and local authorities to the Owakudani sightseeing area was permitted; however, after the detection of local uplift around the no. 39 SPW by InSAR (May 7), the entrance permission was rescinded temporarily on May 8, and a no-entry zone was established inside a 200 m radius from the well (May 11).

On the morning of June 29, Hakone town urgently rescinded permission for the hot spring company to enter the restricted area based on advice of JMA, which considered the seismic surge unusual. The eruption started on June 29; however, crater formation and infrasound signals were not confirmed that day. Thus, the recognition of an eruption was postponed and the eruption was declared by JMA at 12:30 of June 30. At the same time, the VAL was elevated to 3 and residents within 700 m of the vent area, all of whom lived in cottages, were ordered to evacuate.

The VAL was decreased to 2 on September 11, 2015, since inflation of the edifice seemed to have halted since August. The VAL was then decreased to 1 on November 20, 2015; however, since steaming activity continued, the Owakudani sightseeing area remained closed. Operation of the ropeway restarted on April 23, 2016, after gas monitoring and safety measures were established; however, passengers were not allowed to walk out from Owakudani station. Most of the Owakudani sightseeing areas were then opened to the public on July 26, 2016, once further safety procedures were established. However, a part of the sightseeing area and all trails in the younger central cones are still closed at the time of writing, since gas monitoring and safety measures for these areas are still under discussion.

Discussion

Initial phase of the 2015 eruption

The time sequence of the 2015 eruption of Hakone volcano was well observed by geophysical instruments installed around the eruption center; however, its relationship with surface volcanic phenomena is not well known because of very poor visibility. In this and the following sections, we will review the instrumental and visual observations in order to reconstruct the eruption sequence. The reconstructed time sequence is summarized in Fig. 19.

The first direct trigger of the eruption seems to have been by an open crack formation just beneath the eruption center at 7:32 on June 29 as inferred from RTC. At almost the same time, Ground-Based Synthetic Aperture Radar (GBSAR) installed at Owakudani observed that the ground surface near the eruption center started to uplift (Doke et al. 2015). Since the eruption center was formed just above the northern tip of the open crack (Doke et al. 2018; Honda et al. 2015), it is reasonable to assume that the crack created a route for hydrothermal fluid from deep to form the uplift observed by the GBSAR.

On the other hand, seismic observation since the morning of June 29 indicates that the main hypocentral area of the high-frequency seismicity started around a depth of 0 km and gradually propagated deeper (Fig. 16). Thus, the eruption sequence started with shallow crack formation and uplifting of the vent area and was then followed by propagation of high-frequency earthquakes to more than 5 km below sea level taking more than 24 h.

Such a deepening propagation of seismicity contradicts our intuition that assumes the migration of deep hydrothermal fluid toward the surface. We need further theoretical studies to explain the observed seismic propagation; however, at present, we consider that gradual but simultaneous increase in pore pressure within the shallow (< 6 km) hydrothermal system beneath Hakone

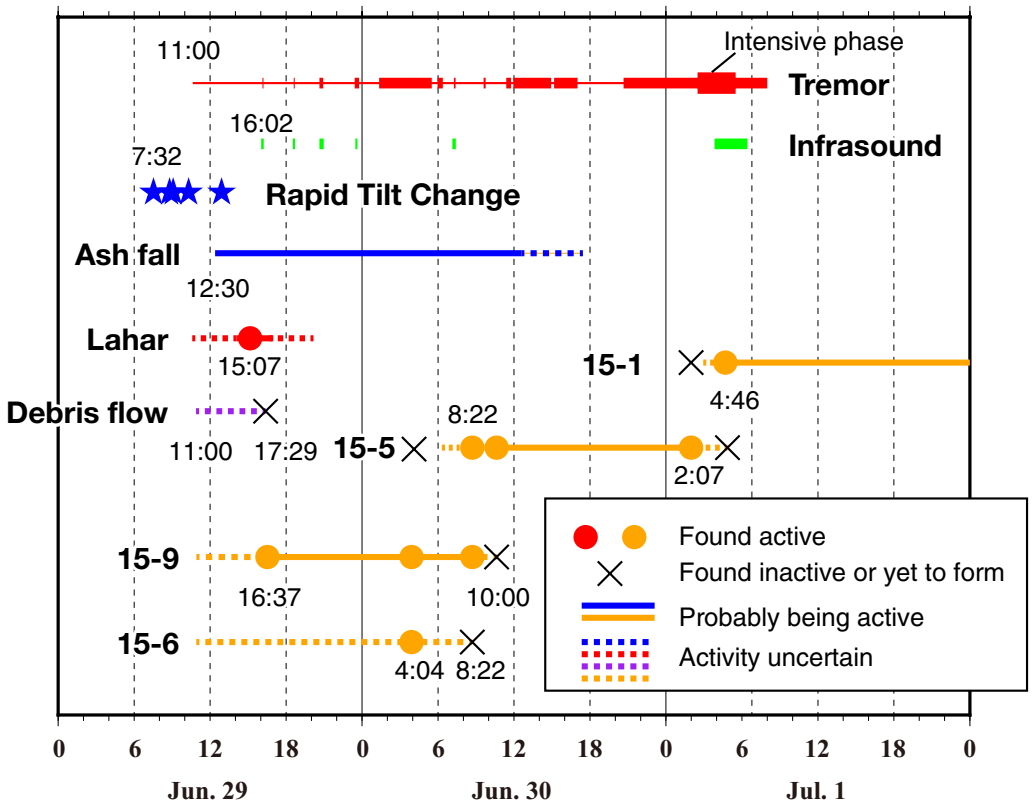

Fig. 19 Time sequence of the 2015 Hakone eruption. The first signal observed was a rapid tilt change (RTC) at 7:32 on June 29. Erosion of the stream bed, probably due to lahar and/or debris flow, tremor, ash fall and infrasound followed. Note that activity at craters relayed as new craters formed and at the last timing of relay, intensive phases of tremor and infrasound were observed

volcano, in which fluid pores are well connected, can be a model to explain the seismic propagation. In such a system, pore pressure of the entire system increases swiftly when it connects to a more pressured hydrothermal system in deep, such as that beneath a brittle-ductile boundary (Fournier 1999). When the fault strength is controlled by a uniform frictional coefficient regardless of depth, orientation of the fault activated by a pore pressure rise is more various in shallower (Fig. 20). In this situation, we can expect earlier seismic activation at shallow depths.

Emission of fluid: timing, origin of water and source crater

Although ash emission seemed to start at around 12:30 on June 29, we have no reason to deny outflow of fluid to the surface at the time of the uplift observed by GBSAR (after 7:32). In fact, mud flows and/or debris flows appear to have eroded the streambed and destroyed plumbing pipes installed beneath Stream L prior to 11:00. We thus conclude that fluid probably flowed from the 15-6 and/or 15-9 vent before 11:00 on the 29th. Even after the initial ash loaded eruption plume (12:30), the mud flow continued to travel downslope. Such mud flows, which are discharged simultaneously with eruption plumes, have been observed in other events such as the 2014 Ontake eruption and are termed syneruptive-spouted type lahars (Sasaki et al. 2016). A syneruptive-spouted type lahar is defined as a syneruptive lahar directly overflowed from the crater with no additional water from a snow cap or crater lake contributing to the flow. Other examples observed in Japan are shown in Sasaki et al. (2016); further, the 1980 eruption of Mt. St. Helens (Brantley and Myers 2000) and the 1926 eruption of Tokachi-dake (Uesawa 2014) indicate significant contributions of water from the edifice to lahar generation, even though water from the surface glacier and snow also contributed. We thus need to consider the possibility of lahars in hazard mitigation planning regardless of the hydrological environment of the eruption center (e.g., with or without a crater lake) and season during which the eruption occurs (e.g., with or without snow cover).

It is noteworthy that the water that created the mud flow during the 2015 eruption seems to be ordinary ground water from this region rather than of pure geothermal origin as indicated from chemical components of

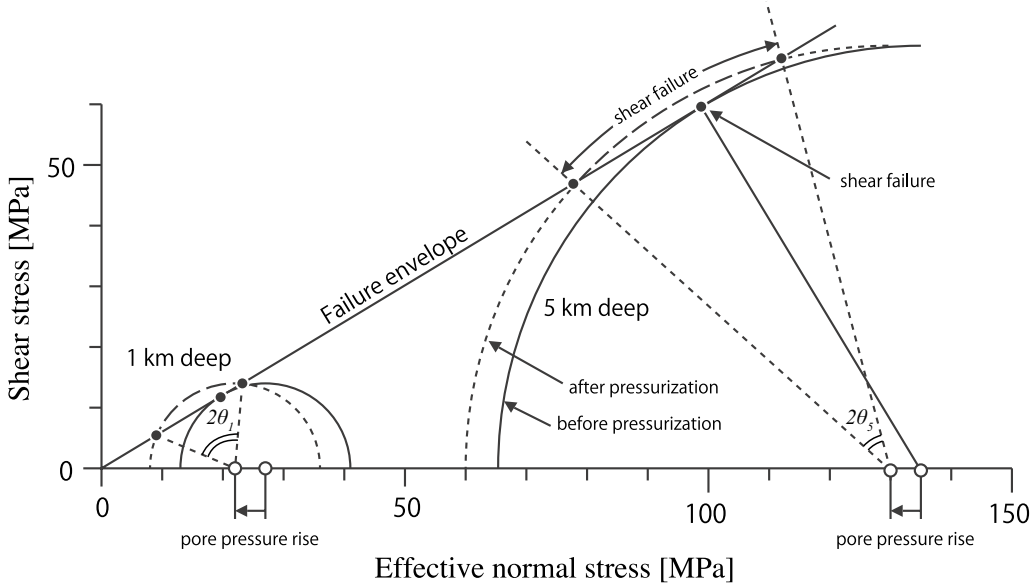

Fig. 20 A conceptual model to explain deepening of seismicity due to pore pressure rise on a Mohr's diagram. A strike slip stress field in which intermediate principal stress is vertical is assumed here. Before a pore pressurization, optimally oriented faults are assumed to be close to shear failure condition regardless of depth since earthquake swarms are ongoing beneath the volcano (< 6 km in depth). After a pore pressure rise, faults are more randomly oriented and are activated to failure throughout the system and a seismic surge commences. However, the orientation range of activated faults is larger in shallower ($\theta_1 > \theta_5$) regions. Thus, the seismicity is more active where shallower and activation in deeper regions needs further pore pressure rise

the water. This fact implies that the water expelled during the eruption was ground water from the vent area, probably purged due to increased hydrothermal pressure at depth. Since onset timings and water chemistries of other syneruptive lahars are not known well, we are not able to discuss the general formation process for such lahars; however, understanding of ground water systems in volcanic edifices will be an important key to assess syneruptive lahar hazards (e.g., Johnson et al. 2018).

The craters were formed one after another in the following 2 days (15-5 on June 30 and 15-1 on July 1) and older craters seemed to be abandoned as new ones formed (Fig. 19). The reason for crater migration toward the west is unclear; however, interestingly, a surge of seismicity at the time of 15-5 formation (Fig. 16) and an intense phase of infrasound and tremor at the time of 15-1 formation (Fig. 19) were observed. Yukutake et al. (2017, 2018) proposed that bursting of gas slugs at the surface of the vent formed the infrasound and tremor observed during the 2015 eruption. Thus, the crater migration that accompanied intensive infrasound and tremor could be triggered by explosive boiling of ascending hydrothermal water in the shallow part of the conduit. Also, the surge of seismicity at the time of 15-5 formation may imply formation of the conduit and further study is needed.

Process behind the volcanic unrest

The 2001 unrest and the 2015 unrest and eruption of Hakone volcano seem to trace an identical course, initiated with inflation of the deep source (≈ 10 km), followed by earthquake swarms and chemical changes of volcanic gases and hot spring waters. In both events, pressure increase in hydrothermal systems beneath the steaming area (≤ 500 m) is implied from blowouts of SPWs in Owakudani.

The minor unrests that took place in 2006, 2008–2009 and 2013 did not show any observable hydrothermal anomalies; however, these unrests also accompanied inflation of the deep source (Harada et al. 2009, 2013; Miyaoka et al. 2011) and some showed temporal increases in the C/S ratio (Ohba et al. 2008) in conjunction with earthquake swarms. These observations imply that volcanic unrest at Hakone is controlled by a common process triggered by deep inflation and subsequent hydrothermal excitation in shallow regions. The 2015 event is not an exception even though it culminated in an eruption. Here we would like to interpret the process behind these events as a response of the hydromagmatic system to sporadic magma replenishment. Before that, the present model for the magma-hydrothermal system beneath Hakone is reviewed.

Figure 21 shows a schematic model of the magma-hydrothermal system inferred from seismic tomography

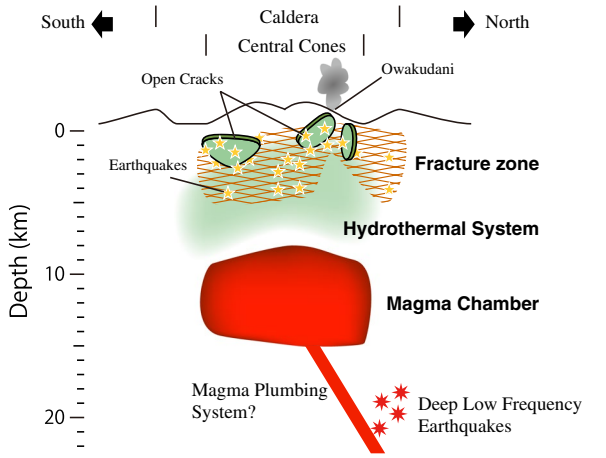

Fig. 21 Schematic model of the magma-hydrothermal system of Hakone volcano inferred from seismic tomography and observation during the 2015 unrest and eruption (after Yukutake et al. 2015). North–south section of the system is shown. Thickness of open cracks is not to scale

and previous studies (Yukutake et al. 2015). The principal magma chamber seems to be located at 10 km or deeper as inferred from a region characterized by low Vp and high Vp/Vs (Yukutake et al. 2015).

Above the magma chamber is a hydrothermal system characterized by low Vp and low Vp/Vs ($\leq$10 km in depth). The hydrothermal system extends to near the surface where steaming activity takes place (e.g., at Owakudani). Above the hydrothermal system is a fractured region where volcano tectonic earthquakes take place ($\leq$6 km in depth). This is the region where earthquake swarms during volcanic unrest occurred and could be partly overlapped with the hydrothermal system. This region could form a mesh structure (Sibson 1996), which is a network composed of tensile cracks and faults around the cracks. The tensile cracks and faults beneath the volcano were observed in previous studies (Yukutake et al. 2010; Daita et al. 2009; Honda et al. 2014).

The process behind the volcanic unrest can be interpreted as follows. Inflation of the deep source ($\approx$10 km) characterizes the very early phase of Hakone unrest. The inflation in deep regions can be interpreted as magma replenishment as the inflation source corresponds to the region of the assumed magma chamber. Also, DLF events that take place in the early phase of inflation could imply migration of magma (Yukutake et al. 2015). During observed events, magma ascent to shallower areas ($<<$10 km) does not seem to have occurred since no migration of earthquakes from deep to shallow, or extensive dike formation, has never been implied by seismic or geodetic observations. Rather, the replenishment of magma to the magma chamber causes increased pressure of pores in the magma-hydrothermal system and triggers a spectrum of volcanic unrest including earthquake swarms, blowout of SPWs and component changes of gas.

The time sequence of earthquake frequency in the events of 2001 and 2015 (Fig. 5) could give an insight to the pressure status of the hydrothermal system. In these events, exponential decay of seismicity was observed after a sharp increase. Such temporal patterns of seismicity were observed during the Matsushiro Earthquake Swarm, in northern part of Nagano prefecture, Japan, from 1965 to 1967 (here after MES) and were interpreted as a step like increase in pore pressure after comparing with a series of experiments of acoustic emission (Mogi 1988). A recent study argues that such exponential decay can be caused by loss of pore pressure rather than pressure being maintained after the initial increase (Ogasawara 2002); however, in any case, seismic changes observed during the 2001 and 2015 events can be interpreted as a rapid ($<$10–20 day) increase in pore pressure caused by magma intrusion and a prolonged process of crustal relaxation following ($<$150–200 days; Fig. 5).

In the case of the MES, seismicity surged three times and each period was followed by an exponential decay; however, at Hakone, exponential decay was observed only once during each unrest. This observation suggests that magma replenishment took place only once per unrest. In addition, the third exponential decay in the MES was interrupted as a "water eruption" that drained pore fluid to the surface. The sudden decrease in seismicity is interpreted as a rapid decrease in pore pressure due to surface drainage (Mogi 1988). At Hakone, such a drastic decrease had never been observed, even after SPW blowout or phreatic eruption. In contrast, the water eruption associated with the MES implied that the eruption and the SPW blowouts in Hakone were not enough to relax pore pressure beneath the volcano significantly.

At Hakone, chemical composition changes of hot spring waters and gases culminated after the 2015 eruption and an aseismic upwelling of hydrothermal fluid long after the eruption was inferred in December 2015 (Fig. 18). This is due to a time lag that reflects transportation in the hydrothermal system. However, since the pressure changes in shallow regions take place within a relatively short period after magma replenishment in deep regions, temperature or some chemical components could change swiftly to reflect hydrological potential; geothermal water or gas that is in equilibrium slightly deeper is transported to the surface, and such change appears in water and steam from some wells. A blowout of steam wells during the unrests in 2001 and 2015 and sudden temperature increase in hot spring water

observed at Gora in the very early phase of the 2001 unrest could be such cases.

Future mitigation measures

Owing to the pre-established evacuation manual and VALs, mitigation measures can be swiftly implemented after recognition of unrest. Urgency is critically important considering a large transient population in Owakudani area (maximum 2800 at lunch time in holiday season) is exposed to the volcanic hazard. The mitigation measures are encouraged by the fact that steaming anomalies and local uplift detected by InSAR indicate the Owakudani area as the most possible eruption center.

However, since open cracks seem to have triggered the eruption in 2015, it could be reasonable to assume that eruptions could happen anywhere on the surface above cracks. Indeed, topographical analyses show several fissure vents in the younger central cone area (Kobayashi et al. 2006). Evolving mitigation measures should consider vent formation in areas where ancient vent opening is evident.

The 2015 eruption seems to have been caused when and where an open crack reached near to the ground surface. Since we cannot forecast the timing, location, nor size of a crack opening, forecasting of eruptions is impossible. This fact indicates that evacuation from the younger central cone area soon after recognition of unrest is the key to hazard mitigation. To avoid false alarm, volcanic unrest needs to be evaluated in a more quantitative manner based on understanding of the overall volcanic process. In addition, monitoring of rapid tilt change, which indicates shallow crack opening, could be critical for early warning systems.

Conclusion

The precursor, eruption and pre-eruptive steaming activity of the 2015 eruption of Hakone volcano were summarized. There was a broad spectrum of precursors including inflation in deep regions, deep low-frequency events, earthquake swarms, tilt change and anomalies of steaming activity. Due to such extensive unrest, hazard mitigation measures were implemented 2 months before the eruption. The swift implementation was helped by the evacuation manual prepared by local governments and the volcano alert level system announced by Japan Meteorological Agency, both of which were established before onset of the 2015 unrest.

Volcanic unrest of Hakone volcano seems to be triggered by magma replenishment to the deep magma chamber and by pore pressure increase in the hydrothermal system beneath the volcano. Geophysical observations around the eruption center imply that the 2015 eruption took place owing to the formation of an open crack that reached near to the ground surface 5 h before the onset of ash fall. After the crack formation, fluid discharge from the source crater likely occurred before the ash emission. However, no signals associated with the ash fall or fluid discharge was observed by geophysical instruments.

Abbreviations

CSAMT: Controlled Source Audio-Frequency Magneto-Telluric; DPC: Disaster Prevention Council for Hakone volcano; HSRI: Hot Springs Research Institute of Kanagawa Prefecture; InSAR: interferometric synthetic-aperture radar; IRI: Industrial Research Institute of Kanagawa Prefecture; JMA: Japan Meteorological Agency; MES: Matsushiro Earthquake Swarm (1965–1967); NFF: newly formed fumaroles; NHF: heat flux due to natural steaming activity on the surface (= not steam well) in Owakudani; RTC: rapid tilt change; SPW: steam production well for making hot spring water in Owakudani; VAL: volcano alert level.

Authors' contributions

KM engaged in geological observation and drafted the manuscript compiling multidisciplinary data. YY determined hypocenter distributions. GK conducted field sampling and chemical analysis of waters in Owakudani. MH processed GNSS data to deduce inflation of the deep source. KI analyzed tiltmeter data. JT conducted field surveys during the eruption with KM. All authors read and approved the final manuscript.

Author details

[1] Hot Springs Research Institute of Kanagawa Prefecture, 586 Iriuda, Odawara, Kanagawa 250-0031, Japan. [2] Japan Meteorological Agency, 1-3-4 Otemachi, Chiyoda, Tokyo 100-8122, Japan.

Acknowledgements

The CSAMT profile was provided by Waterworks Department, Public Enterprise Agency of Kanagawa Prefecture. Heat flux in Owakudani had been observed by Odawara Public Works Center. Industrial Research Institution of Kanagawa Prefecture provided images taken by a web camera after the eruption. Hakone Town Office and Hakone Onsen Kyokyu Co. Ltd helped with field survey. Discussion with Kohichi Uhira (JMA), Mitsuhiro Yoshimoto (MFRI), Masashi Nagai (NIED) and Takeshi Ohba (Tokai Univ.) was beneficial to the study. Minako Shibata patiently reviewed eruption movies and determined timing of crater formation. This manuscript was greatly improved by helpful comment from two anonymous reviewers and Christina Magill (Macquarie Univ.).

Competing interests

The authors declare that they have no competing interests.

Ethics approval and consent to participate

Not applicable.

Funding

This study was implemented as an ordinary research project of HSRI.

Publisher's Note

Received: 10 November 2017 Accepted: 18 April 2018
Published online: 26 April 2018

References

Barberi F, Bertagnini A, Landi P, Principe C (1992) A review on phreatic eruptions and their precursors. J Volcanol Geotherm Res 52:231–246. https://doi.org/10.1016/0377-0273(92)90046-G

Beard KV (1977) Terminal velocity adjustment for cloud and precipitation drops aloft. J Atmos Sci 34:1293–1298

Brantley S, Myers B (2000) Mount St. Helens—from the 1980 eruption to 2000. US Geol Surv Fact Sheet 036–00:1–2

Daita Y, Tanada T, Tanbo T, Ito H, Harada M, Mannen K (2009) Temporal change of the pressure source estimated by tilt records during the 2001 Hakone swarm activity. Bull Volcanol Soc Japan 54:223–234 **(in Japanese with English abstract)**

Doke R, Harada M, Takenaka J, Mannen K (2015) Surface deformation at Owakudani associated with 2015 volcanic activities of Hakone volcano. Programme and abstracts. The Volcanological Society of Japan 2015 fall meeting 41 **(in Japanese)**

Doke R, Harada M, Mannen K, Itadera K, Takenaka J (2018) InSAR analysis for detecting the route of hydrothermal fluid to the surface during the 2015 phreatic eruption of Hakone Volcano, Japan. Earth Planets Space. https://doi.org/10.1186/s40623-018-0834-4

Fournier RO (1999) Hydrothermal processes related to movement of fluid from plastic into brittle rock in the magmatic-epithermal environment. Econ Geol 94:1193–1211. https://doi.org/10.2113/gsecongeo.94.8.1193

Furukawa R, Ishizuka Y, Yamasaki S, Mannen K, Nagai M, Miwa T, Yoshimoto M, Tsunematsu K, Uchiyama T, Baba A (2015) Pyroclastic fall deposit of 2015 eruption from Hakone volcano, Japan. Programme and abstracts. The Volcanological Society of Japan 2015 fall meeting 191 **(in Japanese)**

Hakamata K, Sugiyama S, Imanaga I, Mannen K, Oki Y (2005) K-Ar ages of Hakone Volcano, Japan. Bull Volcanol Soc Japan 50:285–299 **(in Japanese with English abstract)**

Harada M, Kobayashi A, Hosono K, Abstr AY (2009) Crustal deformations around Mt. Hakone and Mt. Fuji since the Hakone swarm activity in 2001. Bull Hot Springs Res Inst Kanagawa Prefect 41:7–14 **(in Japanese with English abstract)**

Harada M, Odawara K, Matsuzawa S, Daita Y, Itadera K, Tanada K (2012) Changes of surface conditions and infrared thermal camera observation at the northern side of Owakudani, Hakone volcano. Bull Hot Springs Res Inst Kanagawa Prefect 44:55–62 **(in Japanese with English abstract)**

Harada M, Yukutake Y, Miyaoka K, Honda R, Itadera K, Doke R, Satomura M, Yoshida A (2013) The classification of earthquake swarm activities in Hakone volcano. Bull Hot Springs Res Inst Kanagawa Prefect 45:1–8 **(in Japanese with English abstract)**

Harada M, Itadera K, Honda R, Yukutake Y, Doke R (2015) Earthquake swarm activities and crustal movements of the 2015 volcanic event at Hakone Volcano (Rapid results). Bull Hot Springs Res Inst Kanagawa Prefect 47:1–10 **(in Japanese with English abstract)**

Honda R, Ito H, Yukutake Y, Harada M, Yoshida A (2011) Features of hypocentral area of swarm earthquakes in Hakone volcano in 1970's revealed by re-analysis using S-P data: comparison with recent activities. Bull Volcanol Soc Japan 56:1–17 **(in Japanese with English abstract)**

Honda R, Yukutake Y, Yoshida A (2014) Stress-induced spatiotemporal variations in anisotropic structures beneath Hakone volcano, Japan, detected by S wave splitting: a tool for volcanic activity monitoring. J Geophys Res Solid Earth 119:7043–7057. https://doi.org/10.1002/2014JB010978

Honda R, Yukutake Y, Harada M, Kato K, Uhira K, Morita Y, Sakai S (2015) Tilt changes and volcanic tremor observed prior to a small eruption of Hakone on 29 June, 2015. Programme and abstracts, The Volcanological Society of Japan 2015 fall meeting 146 **(in Japanese)**

Ishibashi K (1993) Historical earthquake near Odawara, central Japan and their tectonic implications. J Geogr (Chigaku Zasshi) 102:341–353 **(in Japanese with English abstract)**

Johnson PJ, Valentine GA, Stauffer PH et al (2018) Groundwater drainage from fissures as a source for lahars. Bull Volcanol 80:39. https://doi.org/10.1007/s00445-018-1214-4

Jolly AD, Sherburn S, Jousset P, Kilgour G (2010) Eruption source processes derived from seismic and acoustic observations of the 25 September 2007 Ruapehu eruption-North Island, New Zealand. J Volcanol Geotherm Res 191:33–45. https://doi.org/10.1016/j.jvolgeores.2010.01.009

Kato A, Terakawa T, Yamanaka Y, Maeda Y, Horikawa S, Matsuhiro K, Okuda T (2015) Preparatory and precursory processes leading up to the 2014 phreatic eruption of Mount Ontake, Japan. Earth Planets Space 67:111. https://doi.org/10.1186/s40623-015-0288-x

Kobayashi M (1999) Tephrochronology and eruptive activity on Hakone volcano in the past 50 ka. Quat Res 38:327–343 **(in Japanese with English abstract)**

Kobayashi M, Mannen K, Okuno M, Nakamura T, Hakamata K (2006) The Owakidani Tephra Group: a newly discovered post-magmatic eruption product of Hakone Volcano, Japan. Bull Volcanol Soc Japan 51:245–256 **(in Japanese with English abstract)**

Kobayashi T, Morishita Y, Munekane H (2018) First detection of precursory ground inflation of a small phreatic eruption by InSAR. Earth Planet Sci Lett 491:244–254. https://doi.org/10.1016/j.epsl.2018.03.041

Machida H, Arai F (2003) Atlas of Tephra in and around Japan. University of Tokyo Press, Tokyo **(in Japanese)**

Maeno F, Nakada S, Oikawa T, Yoshimoto M, Komori J, Ishizuka Y, Takeshita Y, Shimano T, Kaneko T, Nagai M (2016) Reconstruction of a phreatic eruption on 27 September 2014 at Ontake volcano, central Japan, based on proximal pyroclastic density current and fallout deposits. Earth Planet Space 68:82. https://doi.org/10.1186/s40623-016-0449-6

Mannen K (2003) A re-examination of Hakone Earthquake Swarms by literature (1917-60): implication for the regional tectonics. Bull Volcanol Soc Japan 48:425–443 **(in Japanese with English abstract)**

Mannen K (2008) Hakone Caldera: mode of formation, and role in present-day volcanism. Res Rep Kanagawa Prefect Museum Naturl Hist 13:61–76 **(in Japanese with English abstract)**

Mannen K (2009) Overheated steams in Owakidani fumarolic area: history and cause of extinction. Bull Hot Springs Res Inst Kanagawa Prefect 41:23–32 **(in Japanese with English abstract)**

Miyaoka K, Takagi A (2016) Detection of crustal deformation prior to the 2014 Mt. Ontake eruption by the stacking method. Earth Planets Space 68:60. https://doi.org/10.1186/s40623-016-0439-8

Miyaoka K, Harada M, Doke R (2011) Monitoring of crustal deformation by GNSS data with applying the Stacking method. Bull Hot Springs Res Inst Kanagawa Prefect 46:1–8 **(in Japanese with English abstract)**

Mogi K (1988) The mechanism of the occurrence of the Matsushiro earthquake swarm in central Japan and its relation to the 1964 Niigata earthquake. Tectonophysics 159:109–119. https://doi.org/10.1016/0040-1951(89)90173-X

Murase M, Kimata F, Yamanaka Y, Horikawa S, Matsuhiro K, Matsushima T, Mori H, Ohkura T, Yoshikawa S, Miyajima R, Inoue H, Mishima T, Sonoda T, Uchida K, Yamamoto K, Nakamichi H (2016) Preparatory process preceding the 2014 eruption of Mount Ontake volcano, Japan: insights from precise leveling measurements. Earth Planets Space 68:9. https://doi.org/10.1186/s40623-016-0386-4

Nakamura S (1917) On earthquakes in Hakone. J Meteorol Soc Jpn 36:67–76 **(in Japanese)**

Ogasawara H (2002) A simple analogue experiment to account for power-law and exponential decays of earthquake sequences. Pure Appl Geophys 159:309–343. https://doi.org/10.1007/PL00001255

Ohba T, Daita Y, Sawa T, Taira N, Kakuage Y (2008) Temporal variation in the composition of volcanic gases at Owakudani geothermal area developed on the central cones of Hakone volcano caldera. Bull Hot Springs Res Inst Kanagawa Prefect 40:1–10 **(in Japanese with English abstract)**

Oikawa T, Ishizuka O (2011) Geology of the Atami district. Quadrangle Series, 1:50,000, Geological Survey of Japan, AIST **(in Japanese with English abstract)**

Omori F (1917) On rumblings of Mt. Hakone (sequel). Toyo Gakugei Zasshi 34:203–210 **(in Japanese)**

Sasaki H, Chiba T, Kishimoto H, Naruke S (2016) Characteristics of the syneruptive-spouted type lahar generated by the September 2014 eruption of Mount Ontake, Japan. Earth Planets Space 68:141. https://doi.org/10.1186/s40623-016-0516-z

Sibson RH (1996) Structural permeability of fluid-driven fault-fracture meshes. J Struct Geol 18:1031–1042. https://doi.org/10.1016/0191-8141(96)00032-6

Sugiyama S, Odaka S, Oyama M, Oki Y (1985) Geothermal study for prevention of landslide in Owaki-dani Solfataric Area, Hakone, 1984. Bull Hot Springs Res Inst Kanagawa Prefect 16:225–236 **(in Japanese)**

Tsuchiya M, Mannen K, Kobayashi M, Fukuoka T (2017) Two types of glass shards within the Owakidani Tephra Group Deposit, Hakone Volcano: constraints on their sources and ages. Bull Volcanol Soc Japan 62:23–30 **(in Japanese with English abstract)**

Tsujiuchi W, Suzuki M, Awaya T (2003) Blow out of steam well at Owakudani in 2001. Catfish Lett Hot Springs Res Inst Kanagawa Prefect 53:1–12 **(in Japanese)**

Uesawa S (2014) A study of the Taisho lahar generated by the 1926 eruption of Tokachidake Volcano, central Hokkaido, Japan, and implications for

the generation of cohesive lahars. J Volcanol Geotherm Res 270:23–34. https://doi.org/10.1016/j.jvolgeores.2013.11.002
Usami T (2003) Materials for comprehensive list of destructive earth-quakes in Japan. University of Tokyo Press, Tokyo **(in Japanese)**
Yamasato H, Funasaki J, Takagi Y (2013) The Japan Meteorological Agency's volcanic disaster mitigation initiatives. Tech Note Natl Res Inst Earth Sci Disaster Prev 101–107
Yukutake Y, Tanada T, Honda R, Harada M, Ito H, Yoshida A (2010) Fine fracture structures in the geothermal region of Hakone volcano, revealed by well-resolved earthquake hypocenters and focal mechanisms. Tectonophysics 489:104–118
Yukutake Y, Honda R, Harada M, Aketagawa T, Ito H, Yoshida A (2011a) Remotely-triggered seismicity in the Hakone volcano following the 2011 off the Pacific coast of Tohoku Earthquake. Earth Planets Space 63:737–740. https://doi.org/10.5047/eps.2011.05.004
Yukutake Y, Ito H, Honda R, Harada M, Tanada K, Yoshida A (2011b) Fluid-induced swarm earthquake sequence revealed by precisely determined hypocenters and focal mechanisms in the 2009 activity at Hakone volcano, Japan. J Geophys Res Solid Earth 116:1–13. https://doi.org/10.1029/2010JB008036
Yukutake Y, Honda R, Harada M, Arai R, Matsubara M (2015) A magma-hydrothermal system beneath Hakone volcano, central Japan, revealed by highly resolved velocity structures. J Geophys Res Solid Earth 120:3293–3308. https://doi.org/10.1002/2014JB011856
Yukutake Y, Honda R, Harada M, Doke R, Saito T, Ueno T, Sakai S, Morita Y (2017) Continuous volcanic tremor during the 2015 phreatic eruption in Hakone volcano. Earth Planets Space. https://doi.org/10.1186/s40623-017-0751-y
Yukutake Y, Ichihara M, Honda R (2018) Infrasonic wave accompanying a crack opening during the 2015 Hakone eruption. Earth Planets Space. https://doi.org/10.1186/s40623-018-0820-x